Annals of Mathematical Sciences and Applications
Volume 3, Number 1, 49–88, 2018

A second order free discontinuity model for bituminous surfacing crack recovery and analysis of a nonlocal version of it

Noémie Debroux*, Carole Le Guyader*, and Luminita Vese

We consider a second order variational model dedicated to crack detection on bituminous surfacing. It is based on a variant of the weak formulation of the Blake-Zisserman functional that involves the discontinuity set of the gradient of the unknown, set that encodes the geometrical thin structures we aim to recover, as suggested by Drogoul et al. Following Ambrosio, Faina and March, an approximation of this cost function by elliptic functionals is provided. Theoretical results including existence of minimizers, existence of a unique viscosity solution to the derived evolution problem, and a Γ-convergence result relating the elliptic functionals to the initial weak formulation are given. Extending then the ideas developed in the case of first order nonlocal regularization to higher order derivatives, we provide and analyze a nonlocal version of the model.

AMS 2000 subject classifications: Primary 45E, 49J, 68U10; secondary 35D40, 65D18.
Keywords and phrases: Blake-Zisserman functional, space of generalized special functions of bounded variation ($GSBV$), elliptic approximations, $G(\mathbb{R}^2)$-space of oscillating functions, infinity Laplacian, viscosity solutions, Γ-convergence, convergence analysis, partial minimizer, nonlocal second order operators, fractional Sobolev space, tempered distributions, Fourier transform, fine structure segmentation.

1. Introduction

The scope of this paper is to propose a novel variational method to detect thin structures, namely cracks on bituminous surfacing. If singularities related to edges are classically associated with a discontinuity of gray level

*The project is co-financed by the European Union with the European regional development fund (ERDF, HN0002137) and by the Normandie Regional Council via the M2NUM project. The authors would like to thank Denis Jouin and Cyrille Fauchard (CEREMA, France) for providing the bituminous surfacing images.

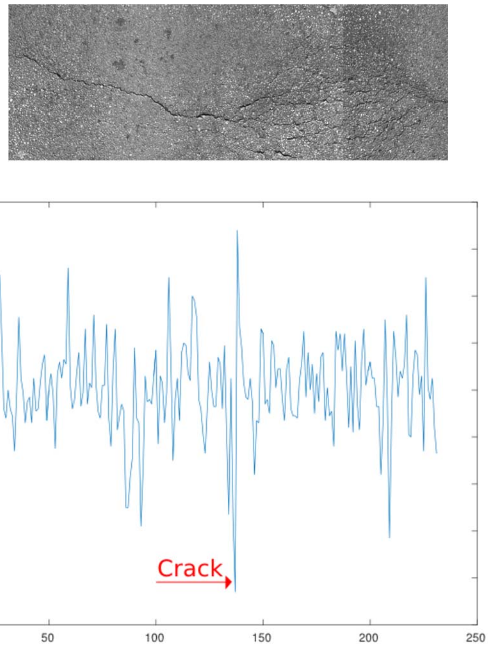

Figure 1: A bituminous surfacing image and a crossplot going through the crack.

intensities across edges (and are thus detected using spatial gradient information carried by the image), this characterization proves to be unsuitable when dealing with points, cracks, or filaments. Indeed, while for an edge the singularity is associated with a jump of the intensity across this edge, for filaments, such a jump does not occur (see [29, p. 2]). As an illustration, on the crossplot of Fig. 1, the crack is represented by a very thin peak and so the spatial gradient is unable to seize this singularity. In [29], Drogoul provides a heuristic illustration of this fact by considering an approximation of the 1D function defined by $f(x) = 0$ if $x \neq 0$ and $f(0) = 1$ as follows: $f_\eta(x) = 0$ if $|x| \geq \eta$ and $f_\eta(x) = \frac{2}{\eta^3}|x|^3 - \frac{3}{\eta^2}|x|^2 + 1$ if $|x| \leq \eta$. It is not difficult to see that $f'_\eta(0) = 0$, showing that the differential operator of order 1 does not capture the singularity at 0. On the other hand, as $f''_\eta(0) = -\frac{6}{\eta^2}$, f''_η clearly exhibits a singularity at 0 when η becomes small. This exemplifies the fact that in order to detect fine structures or filaments, higher order differential operators should be considered. This intuitive illustration is then mathematically formalized in 2D in [29] through Lemma 2.1, and states in substance the following: assuming that a crack can be modelled by an indicator function supported by a smooth curve Γ, it can be approximated by a sequence of smooth functions whose Hessian matrices blow up in the perpendicular direction to Γ, while their gradient is null. Motivated by these observations showing that a suitable model should involve higher order derivatives, the crack recovery model we propose falls within second order variational models. It is based on the Blake-Zisserman functional (see [14]) (recalled in (1)) for computer vision problems that depends on free discontinuities, free gradient discontinuities and second order derivatives, and more precisely, on its approximation by elliptic functionals defined on Sobolev spaces ([4]) —(note that the Blake-Zisserman functional was successfully applied to segmentation as in [42] for the segmentation of a digital model of a mixed urban-agricultural area, or image inpainting as in [21])—. This approximation appears as the counterpart for the second order case of the elliptic approximations designed by Ambrosio and Tortorelli ([2, 3]) to approximate Mumford-Shah functional ([34]), and takes place in a variational sense, namely, the De Giorgi Γ-convergence. The qualifying terms "free discontinuities", "free gradient discontinuities" mean that the functional is minimized over three variables: two unknown sets K_0, K_1 with $K_0 \cup K_1$ closed, and u, a smooth function on $\Omega\backslash(K_0 \cup K_1)$ as follows

$$\begin{aligned} F(u, K_0, K_1) = &\int_{\Omega\backslash(K_0\cup K_1)} \left(|\nabla^2 u|^2 + \Phi(x,u)\right)\, dx \\ &+ \alpha\, \mathcal{H}^{n-1}(K_0 \cap \Omega) + \beta\, \mathcal{H}^{n-1}((K_1\backslash K_0)\cap\Omega), \end{aligned} \tag{1}$$

α and β being two positive parameters. The set K_0 represents the set of jump points for u, and $K_1\backslash K_0$ is the set of crease points of u, those points where u is continuous but ∇u is not. Under certain conditions, the existence of minimizers for Blake-Zisserman functional is ensured over the space $\left\{u : \Omega \subset \mathbb{R}^n \to \mathbb{R} \,|\, u \in L^2(\Omega),\, u \in GSBV(\Omega),\, \nabla u \in (GSBV(\Omega))^n\right\}$, based on a weak formulation of the problem ($GSBV(\Omega)$ being the space of generalized special functions of bounded variation), see [20]. Ambrosio, Faina and March ([4]) introduce a family of elliptic functionals defined on Sobolev spaces, with in particular, a variable encoding the discontinuity set of ∇u which is exactly the structure we aim to recover. This family of functionals is defined by

$$\begin{aligned} F_\varepsilon(u, s, \sigma) = &\int_\Omega \left(\sigma^2 + \kappa_\varepsilon\right) |\nabla^2 u|^2\, dx + \int_\Omega \Phi(x,u)\, dx + (\alpha - \beta)\, \mathcal{G}_\varepsilon(s) \\ &+ \beta\, \mathcal{G}_\varepsilon(\sigma) + \xi_\varepsilon \int_\Omega \left(s^2 + \zeta_\varepsilon\right)\, |\nabla u|^2\, dx, \end{aligned} \tag{2}$$

for suitable infinitesimals κ_ε, ξ_ε and ζ_ε, and with $\mathcal{G}_\varepsilon(l) = \int_\Omega [\varepsilon |\nabla l|^2 + \frac{(l-1)^2}{4\varepsilon}]dx$.

Before depicting in depth the proposed model and its relation to (2), we review some prior related works dedicated to thin pattern recovery. In [9, 29], Aubert and Drogoul introduce a topological-gradient-based method for the detection of fine structures in 2D. Given a PDE depending on a domain Ω, and u_Ω the solution of this PDE, topological asymptotic methods aim to study the variations of a cost function $j(\Omega) = j(\Omega, u_\Omega)$ when a topological modification such as the creation of a small hole or a crack measured by a parameter ϵ is applied to the domain Ω, resulting in Ω_ϵ. The expansion of $j(\Omega_\epsilon)$ with respect to ϵ shows that if one intends to minimize $j(\Omega_\epsilon)$, it is relevant to create holes or cracks at points x_0 where the topological gradient is the most negative. Aubert and Drogoul motivate the construction of their cost function involving second order derivatives by showing that a filament can be approximated by a sequence of smooth functions whose Hessian matrices blow up in the perpendicular direction to the filament, while their gradient is null as already mentioned. The proposed cost function is inspired by the Kirchhoff thin static plate model subject to pure bending with a Poisson ratio $\nu = 0$. A major difference with our model lies in the introduction of a variable that encodes the crack-type singularities. In [12], Bergounioux and Vicente propose a variational model to perform the segmentation of tube-like structures with small diameter in MRI images. It is derived from the Mumford-Shah functional (more precisely, on its approximation by elliptic functionals) and includes geometrical priors prescribing the topology of the solution (tube-like structures defined by thickening a parameterized curve to get a symmetric object of diameter $\alpha > 0$). The keypoint is that the 2D/3D problems involved are equivalent to 1D ones formulated in a weighted Sobolev space where the weight is related to the geometry of the tube. A limitation of this model is that it does not handle junctions of tubes. For another method dedicated to the detection and completion of fine structures in an image and relying on tubular structures, we refer to [35].

Other variational models have been investigated, dedicated to particular applications. In [37], Rochery et al. aim to track thin long objects, with applications to the automatic extraction of road networks in remote sensing images. They propose interesting nonlocal regularizers that enforce straightness on the sought parameterized curve. In [10], Baudour et al. propose a new algorithm for the detection and completion of thin filaments (defined as structures of codimension $n-1$ in an ambient space of dimension n) in noisy blurred 2D or 3D images. To detect such structures, the authors build a 3D vector field lying in the orthogonal plane to the filament, while the completion phase relies on the minimization of a Ginzburg-Landau energy. In [6], Aubert et al. propose detecting image singularities of codimension greater or equal to 2, inspired again by Ginzburg-Landau models.

The spectrum of the methods that address the issue of fine structure recovery is of course not limited to variational ones. Morphological approaches can be found in [41] for automatic detection of vessel-like patterns, but prove to be sensitive to the noise type and time-consuming, as well as wavelet methods. In [39], stochastic methods are developed in which a thin network is simulated by a point process penalizing disconnected segments and favoring aligned pieces.

The next section is dedicated to the depiction of our modelling and its numerical analysis, encompassing existence of minimizers, existence of a unique viscosity solution to the resulting evolution equation, Γ-convergence results and convergence analysis, as well as the derivation of a nonlocal version of it (section 3).

2. Local mathematical modelling and analysis

2.1. Model

Let Ω be a connected bounded open subset of $\mathbb{R}^2$ of class $\mathcal{C}^1$. Let us denote by $f : \bar{\Omega} \to \mathbb{R}$ the 2D image representing bituminous surfacing assumed to be in $L^\infty(\Omega)$. Such an image naturally exhibits dense and highly oscillatory texture, reflecting its intrinsic nonlocal nature. This oscillatory component, although relevant in many applications since providing details and making the image more realistic, proves to be unnecessary for the task to accomplish. This observation motivates the introduction of a mixed decomposition/thin-structure-recognition model in which the crack recovery process operates only on that component of the image denoted by u that does not contain these small features captured in v. A geometrical justification relies on the notion of scale. Cracks on bituminous surfacing can be compared to long and thin filaments displaying junctions. The scale of such structures (the geometric scale of an object being basically the ratio of an area divided by a perimeter) differs from the scale of small oscillatory patterns present in the image: if the image domain is the $n \times n$ discretized unit square and if, for the sake of simplicity and as an illustration, the crack is modelled as a rectangle of $1 \times k$ pixels with $k \gg 1$, its scale behaves like $\frac{1}{2n}$, while a small feature of a pixel size will have a scale of $\frac{1}{4n}$, so twice as less. By choosing accurately the parameters involved in the modelling, these two features can be properly discriminated: small-scale features related to texture will be removed and captured by component v, while larger-scale features such as cracks will be kept in u. In [33], Meyer introduces the space $G(\mathbb{R}^2)$ (he works on $\mathbb{R}^2$ to remove the problem of boundary conditions) of distributions v that can be written as $v = \operatorname{div} \vec{g}$, where $\vec{g} = (g_1, g_2) \in \left(L^\infty(\mathbb{R}^2)\right)^2$, and equipped with the norm defined by

$$\|v\|_{G(\mathbb{R}^2)} = \inf \left\{ \|\sqrt{g_1^2 + g_2^2}\|_{L^\infty(\mathbb{R}^2)}, \mid v = \operatorname{div} \vec{g} \right\} \tag{3}$$

to capture the oscillatory nature of texture (highly oscillatory patterns have a small G-norm). A further justification of the use of this space is the link between the G-norm and the notion of scale provided by Strang ([40]): if $v \in G$, then $\|v\|_G = \sup\limits_{E \subset \Omega} \frac{\int_E v}{P(E,\Omega)}$, with Ω the image domain and $P(E,\Omega)$ denoting the perimeter of E in Ω, showing that the stronger the penalization of $\|v\|_G$ is, the smaller the scale of the details kept in v is. Although mathematically relevant (as it resembles the dual space of BV), the G-space is hard to handle from a numerical point of view. To approximate the G-norm, we introduce an auxiliary variable that naturally stems from the Helmholtz-Hodge decomposition as follows: $\vec{g} = \nabla Q + \vec{P}$, with $\vec{P}$ a divergence-free vector that we disregard afterwards. The coupling between $\vec{g}$ and ∇Q is achieved through a quadratic penalization and the minimization of the L^∞-norm is now applied to ∇Q, yielding a problem related to the absolutely minimizing Lipschitz extensions and to the infinity Laplacian.

Equipped with this material, we propose, in a single variational framework, a mixed decomposition/free discontinuity and free gradient discontinuity model, first in its weak formulation, $\mathcal{H}^1$ denoting the Hausdorff 1-dimensional measure

$$\begin{aligned} \inf \bar{F}(u, \vec{g}, Q) = {} & \|f - u - \operatorname{div} \vec{g}\|^2_{L^2(\Omega)} + \mu\, \||\nabla Q|\|_{L^\infty(\Omega)} + \frac{\gamma}{2}\, \||\vec{g} - \nabla Q|\|^2_{L^2(\Omega)} \\ & + \rho \int_\Omega |\nabla^2 u|^2\, dx + (\alpha - \beta)\, \mathcal{H}^1(S_u) + \beta\, \mathcal{H}^1(S_{\nabla u} \backslash S_u), \end{aligned} \tag{4}$$

$\nabla^2 u$ being the Hessian matrix, and with ∇u denoting the approximate differential, S_u, the discontinuity set of u, and $S_{\nabla u}$, the discontinuity set of ∇u. The three first penalizing terms are related to the decomposition of f into $u + v$ with v belonging to G, while the last components are devoted to the crack detection process. The component $\int_\Omega |\nabla^2 u|^2\, dx$ enables us to control the smoothness of u, while the remaining components monitor the size of the jump/crease sets. Second, phrased in terms of elliptic functionals inspired by [4], with two new auxiliary variables v_1 and v_2 encoding respectively the set of jumps of u and the set of jumps of ∇u, with $\mathcal{G}_\varepsilon$ defined above, and with suitable infinitesimals κ_ε, ξ_ε and ζ_ε

$$\begin{aligned}\inf \mathcal{F}_\varepsilon(u,\vec{g},Q,v_1,v_2) = \; & \|f-u-\operatorname{div}\vec{g}\|^2_{L^2(\Omega)} + \mu\,\||\nabla Q|\|_{L^\infty(\Omega)} \\ & + \frac{\gamma}{2}\,\||\vec{g}-\nabla Q|\|^2_{L^2(\Omega)} + \rho\int_\Omega (v_2^2+\kappa_\varepsilon)\,|\nabla^2 u|^2\,dx \\ & + \xi_\varepsilon\int_\Omega (v_1^2+\zeta_\epsilon)\,|\nabla u|^2\,dx + (\alpha-\beta)\,\mathcal{G}_\varepsilon(v_1) + \beta\,\mathcal{G}_\varepsilon(v_2).\end{aligned} \tag{5}$$

The different parameters are introduced in order to properly discriminate small features (related to the intrinsic oscillatory nature of the image) from larger scale features such as cracks, and to properly fit the characteristics of the minimizers. The component $\|f-u-\operatorname{div}\vec{g}\|^2_{L^2(\Omega)}$ forces the original image to be close to $u+\operatorname{div}\vec{g}$ with appropriate smoothness on u, and $v=\operatorname{div}\vec{g}$ lives in a suitable functional space. Indeed, if $\gamma\to+\infty$, we formally get $f\simeq u+\operatorname{div}\vec{g}$ with $\vec{g}\in(L^\infty(\Omega))^2$. The variable v_1 (resp. v_2) with range $[0,1]$ is related to the set of jumps (resp. creases). A minimizing $v_{1,\varepsilon}$ (resp. $v_{2,\varepsilon}$) is in particular close to 0 in a neighborhood of the jump (resp. crease) set, and far from it, is close to 1. Function u is thus a smooth approximation of the observed f, this smoothing effect being localized only on homogeneous parts. The representation of each auxiliary variable forms a partition of the data. Now looking closer at the components $\int_\Omega (v_2^2+\kappa_\varepsilon)\,|\nabla^2 u|^2\,dx$ and $\mathcal{G}_\varepsilon(v_2)$, letting ε become small induces that v_2 should be 1 almost everywhere on Ω, except where $|\nabla^2 u|^2$ blows up. This observation supports the crack characterization we gave, and ensures that v_2 encodes the structures we aim to recover.

We now provide several theoretical results.

2.2. Existence of minimizers

Theorem 1. *With $\kappa_\varepsilon,\xi_\varepsilon,\zeta_\varepsilon>0$, problem (5) admits minimizers $(u=u_\varepsilon,\vec{g}=\vec{g_\varepsilon},Q=Q_\varepsilon,v_1=v_{1,\varepsilon},v_2=v_{2,\varepsilon})$ on $\{u\in W^{2,2}(\Omega)\,|\,\int_\Omega u\,dx=\int_\Omega f\,dx\}\times H(div)\times\{Q\in W^{1,\infty}(\Omega)\,|\,\int_\Omega Q\,dx=0\}\times W^{1,2}(\Omega,[0,1])\times W^{1,2}(\Omega,[0,1])$, with $H(div)$, the Hilbert space defined by $H(div)=\{\sigma\in(L^2(\Omega))^2\,|\,div\,\sigma\in L^2(\Omega)\}$ endowed with the inner product*

$$\langle\vec{\sigma_1},\vec{\sigma_2}\rangle_{H(div)} := \langle\vec{\sigma_1},\vec{\sigma_2}\rangle_{(L^2(\Omega))^2} + \langle div\,\vec{\sigma_1}, div\,\vec{\sigma_2}\rangle_{L^2(\Omega)},$$

$\forall(\vec{\sigma_1},\vec{\sigma_2})\in(H(div))^2$.

Remark 1. *Condition $\int_\Omega Q\,dx = 0$ is not restrictive. An argument to include the constraint $\int_\Omega u\,dx = \int_\Omega f\,dx$ is that the space $G(\Omega)$ defined by $G(\Omega) = \{v \in L^2(\Omega)\,|\, v = div\,\vec{g},\ \vec{g} \in L^\infty(\Omega, \mathbb{R}^2),\ \vec{g}\cdot\vec{n} = 0 \text{ on } \partial\Omega\}$ coincides with the space $\{v \in L^2(\Omega)\,|\, \int_\Omega v\,dx = 0\}$ (see [7, Proposition 2.1]).*

Proof. The proof is based on Poincaré-Wirtinger inequality as well as a result by Berkovitz ([13, Theorem 1]) that states in substance that under suitable conditions on h, the integral functional $I(y,z) = \int_\Omega h(t, y(t), z(t))\,d\mu$ is lower semicontinuous with respect to the joint strong convergence of $y_k \to y$ in $L^p(\Omega)$ and weak convergence of $z_k \rightharpoonup z$ in $L^q(\Omega)$, $1 \le p, q \le \infty$ (with $\Omega \subset \mathbb{R}^n$ bounded open set). □

Remark 2. *It is possible to set $\xi_\varepsilon = 0$ in (5) (the existence theorem still holds), but a suitable functional space for u becomes $W^{2,2}_{loc}(\Omega) \cap L^\infty(\Omega)$. For instance, with the condition $\|u\|_{L^\infty(\Omega)} \le \|f\|_{L^\infty(\Omega)}$, which is reasonable in virtue of the smoothing properties of the functional. Indeed, [4, Proposition 4.6] provides a uniform bound on $\|\nabla u\|_{L^2(A)}$ once a uniform bound is extracted for $\|u\|_{L^2(B)}$ and $\|\nabla^2 u\|_{L^2(B)}$ with $A, B \subset \mathbb{R}^2$ open sets and $(A_{2r}) \subsetneq B$.*

Remark 3. *The case $\kappa_\varepsilon = 0$ can also be considered (an existence theorem still holds) but requires more care and applies to a problem no longer phrased in terms of a L^2-penalization for ∇u, but with a L^γ-penalization, $\gamma > 2$. The unknown u should be searched in the subspace of $W^{1,2}(\Omega)$ defined by $\{u \in W^{1,2}(\Omega)\,|\, v_2\nabla u \in W^{1,p}(\Omega, \mathbb{R}^2)\}$, with $p = \frac{2\gamma}{\gamma+2} \in]1, 2[$. The boundedness of v_2 in $W^{1,2}(\Omega)$ as well as the boundedness of $|\nabla u|$ in $L^\gamma(\Omega)$, and the fact that $\nabla(v_2\,\nabla u) = v_2\,\nabla^2 u + \nabla v_2 \bigotimes \nabla u$ show that $v_2\,\nabla u$ is bounded in $W^{1,p}(\Omega, \mathbb{R}^2)$ using Hölder's inequality.*

Remark 4. *Functional $\mathcal{F}_\varepsilon$ is convex in each variable (which yields a natural alternating framework for the numerical resolution) but not in the joint variable $(u, \vec{g}, Q, v_1, v_2)$. Nevertheless, for v_1, v_2 fixed, if $(u_1, \vec{g_1}, Q_1)$ and $(u_2, \vec{g_2}, Q_2)$ denote two minimizing elements, it can be proved that $u_1 = u_2$ a.e., $div\,\vec{g_1} = div\,\vec{g_2}$ a.e., and $\vec{g_1} - \vec{g_2} = \nabla Q_1 - \nabla Q_2$ a.e.. Consequently, $div\,(\nabla Q_1 - \nabla Q_2) = \Delta(Q_1 - Q_2) \in L^2(\Omega) = 0$ a.e.. By the generalized Green's formula [28, Proposition 3.58], $\int_\Omega |\nabla(Q_1 - Q_2)|^2\,dx = \langle \nabla(Q_1 - Q_2)\cdot\vec{n}, \gamma_0(Q_1 - Q_2)\rangle$, the linear functional $\nabla(Q_1 - Q_2)\cdot\vec{n}$ belonging to the dual $H^{-1/2}(\partial\Omega)$ of the space of traces $H^{1/2}(\partial\Omega)$. If we assume that $\nabla(Q_1 - Q_2)\cdot\vec{n} = 0$ on $\partial\Omega$, then $Q_1 = Q_2$ a.e..*

2.3. Existence of solutions for the Euler-Lagrange equations

We now focus on the elliptic functional, which is the one we solve in practice. Note that, in the numerical simulations, we have dropped the constants κ_ε and ζ_ε. We first derive the Euler-Lagrange equations according to each unknown, with $x = (x_1, x_2)$ and $\vec{n} = (n_{x_1}, n_{x_2})$, the unit outward normal to the boundary. Making use of the absolutely minimizing Lipschitz extensions ([5]) for the equation in Q, we get:

$$\begin{cases} v_1 = \dfrac{\frac{\alpha-\beta}{2\varepsilon} + 2(\alpha-\beta)\varepsilon\Delta v_1}{2\xi_\varepsilon|\nabla u|^2 + \frac{\alpha-\beta}{2\varepsilon}}, \;\; v_2 = \dfrac{\frac{\beta}{2\varepsilon} + 2\beta\varepsilon\Delta v_2}{2\rho|\nabla^2 u|^2 + \frac{\beta}{2\varepsilon}}, \\ g_1 = \partial_{x_1} Q - \frac{2}{\gamma}\,\partial_{x_1}\left(f - u - \operatorname{div}\vec{g}\right), \;\; g_2 = \partial_{x_2} Q - \frac{2}{\gamma}\,\partial_{x_2}\left(f - u - \operatorname{div}\vec{g}\right), \\ u = (f - \operatorname{div}\vec{g}) - \rho\,\frac{\partial^2}{\partial x_1^2}\left(v_2^2\,\frac{\partial^2 u}{\partial x_1^2}\right) - \rho\,\frac{\partial^2}{\partial x_2^2}\left(v_2^2\,\frac{\partial^2 u}{\partial x_2^2}\right) \\ -2\rho\,\frac{\partial^2}{\partial x_1\partial x_2}\left(v_2^2\,\frac{\partial^2 u}{\partial x_1\partial x_2}\right) + \xi_\varepsilon \operatorname{div}\left(v_1^2\,\nabla u\right), \\ -\mu\Delta_\infty Q - \gamma\Delta Q + \gamma\operatorname{div}\vec{g} = 0, \end{cases}$$

combined with the boundary conditions $\nabla v_1 \cdot \vec{n} = 0$, $\nabla v_2 \cdot \vec{n} = 0$, $(f - u - \operatorname{div}\vec{g})n_{x_1} = 0$, $(f - u - \operatorname{div}\vec{g})n_{x_2} = 0$, $v_1^2\nabla u \cdot \vec{n} = 0$, $v_2^2\partial^2_{x_1x_1} u\, n_{x_1} = 0$, $\partial_{x_1}\left(v_2^2\partial^2_{x_1x_1}u\right) n_{x_1} = 0$, $v_2^2\partial^2_{x_2x_2}u\; n_{x_2} = 0$, $\partial_{x_2}\left(v_2^2\partial^2_{x_2x_2}u\right) n_{x_2} = 0$, $v_2^2\partial^2_{x_1x_2}u\; n_{x_1} = 0$, $\partial_{x_1}\left(v_2^2\partial^2_{x_1x_2}u\right) n_{x_2} = 0$ and $(\vec{g} - \nabla Q)\cdot\vec{n} = 0$ on $\partial\Omega$. Let us now embed the last equation in a time-dependent setting. Let $T > 0$ be given. The evolution equation in the unknown Q is thus given by

$$\text{(EE)} \qquad \begin{cases} \dfrac{\partial Q}{\partial t} = \mu\Delta_\infty Q + \gamma\Delta Q - \gamma\operatorname{div}\vec{g} \text{ on } \mathbb{R}^2 \times (0, T), \\ Q(x, 0) = Q_0(x) \text{ on } \mathbb{R}^2, \end{cases}$$

with $Q_0 \in W^{1,\infty}(\mathbb{R}^2)$ and B_0 its Lipschitz constant. (To remove the problem of boundary conditions, we work on $\mathbb{R}^2$ for the spatial domain). We now give an existence/uniqueness result for the PDE in Q in the viscosity solution theory framework. To do so, we first need the additional following assumption

(H) $\operatorname{div}\vec{g}$ is bounded and is Lipschitz continuous uniformly in time with $\kappa_{\vec{g}}$ its Lipschitz constant independant of time.

For the sake of conciseness, the evolution equation is now written in the form

$$\frac{\partial Q}{\partial t} + G(x, t, \nabla Q, \nabla^2 Q) = 0,$$

with $G : \mathbb{R}^2 \times [0,T) \times \mathbb{R}^2 \times \mathcal{S}^2$ ($\mathcal{S}^2$ being the set of symmetric 2×2 matrices equipped with its natural partial order) defined by

$$\begin{aligned} G(x,t,\vec{p},X) &= -\gamma \text{trace}(X) - \mu \text{trace}(\frac{\vec{p} \otimes \vec{p}}{|\vec{p}|^2} X) + \gamma \text{div}\, \vec{g}, \\ &= E(X) + F(\vec{p},X) + \gamma \text{div}\, \vec{g}, \end{aligned}$$

and with the following properties

1. The operators G, $E : X \mapsto -\gamma \text{trace}(X)$ and $F : (\vec{p},X) \mapsto -\mu\, \text{trace}\big(\frac{\vec{p}\otimes\vec{p}}{|\vec{p}|^2} X\big)$ are independent of Q and are elliptic, *i.e.* $\forall X, Y \in \mathcal{S}^2$, $\forall \vec{p} \in \mathbb{R}^2 \setminus \{\vec{0}_{\mathbb{R}^2}\}$, if $X \leq Y$ then $F(\vec{p},X) \geq F(\vec{p},Y)$.
2. F is locally bounded on $\mathbb{R}^2 \times \mathcal{S}^2$, continuous on $\mathbb{R}^2 \setminus \{\vec{0}_{\mathbb{R}^2}\} \times \mathcal{S}^2$, and $F^*(0,0) = F_*(0,0) = 0$, where F^* (resp. F_*) is the upper semicontinuous (usc) envelope (resp. lower semicontinuous (lsc) envelope) of F. Indeed, using Rayleigh quotient, it is not difficult to see that for nonzero vector $\vec{p}$, $\lambda_{min}(X) \leq \text{trace}\left(\frac{\vec{p}\otimes\vec{p}}{|\vec{p}|^2} X\right) \leq \lambda_{max}(X)$, λ_{min} (resp. λ_{max}) denoting the smallest (resp. biggest) eigenvalue of X.

The first important result is a comparison principle, which states that if a sub-solution and a super-solution are ordered at initial time then they are ordered at any time.

Theorem 2 (Comparison principle)**.** *Assume (H) and let* $u : \mathbb{R}^2 \times [0,T) \to \mathbb{R}$ *be a bounded upper semicontinuous sub-solution and* $v : \mathbb{R}^2 \times [0,T) \to \mathbb{R}$ *be a bounded lower semicontinuous super-solution of (EE). Assume that* $u(x,0) \leq Q_0(x) \leq v(x,0)$ *in* $\mathbb{R}^2$*, then* $u \leq v$ *in* $\mathbb{R}^2 \times [0,T)$*.*

Proof. The proof is rather classical and we refer the reader to [30][Definition 4.1] for the definition of viscosity solutions and for additional material. □

We now turn to the existence of a solution. To do so, we use the classical Perron's method and need to construct barriers.

Theorem 3 (Construction of barriers)**.** *Assume (H) and let* $Q_0 \in W^{1,\infty}(\mathbb{R}^2)$*. Then* $u^+ = \sup_{x\in\mathbb{R}^2} Q_0(x) + \gamma \| div\, \vec{g} \|_{L^\infty(\mathbb{R}^2\times[0,T))} t$ *and* $u^- = \inf_{x\in\mathbb{R}^2} Q_0(x) - \gamma \| div\, \vec{g} \|_{L^\infty(\mathbb{R}^2\times[0,T))} t$ *are respectively super- and sub-solution of (EE).*

The proof of this theorem is straightforward. A direct consequence of the two previous results is the following existence theorem.

Theorem 4 (Existence and uniqueness of a solution)**.** *Assume (H) and* $Q_0 \in W^{1,\infty}(\mathbb{R}^2)$*. Then there exists a unique bounded continuous solution of (EE) in* $\mathbb{R}^2 \times [0,T)$*.*

Let us now focus on the regularity of the solution. Let us first consider the regularity in space.

Theorem 5 (Lipschitz regularity in space)**.** *Assume (H) and that* $\|\nabla Q_0\|_{L^\infty(\mathbb{R}^2)} \leq B_0$ *with* $B_0 > 0$*. Then the solution of (EE) is Lipschitz continuous and satisfies*

$$\|\nabla Q(.,t)\|_{L^\infty(\mathbb{R}^2)} \leq B(t),$$

with $B(t) = \gamma \kappa_{\vec{g}} t + B_0$*.*

Besides, we can show that this solution is also uniformly continuous in time.

Theorem 6. *Assume (H), and that* $div\,\vec{g}$ *is uniformly continuous in time with* $\omega_{div\,\vec{g}}$ *its modulus of continuity. Then the solution of (EE) is uniformly continuous in time.*

This concludes this section on the existence of a well-defined and smooth solution of the evolution equation derived for Q. Let us now turn to a Γ-convergence result.

2.4. Asymptotic results

In that purpose, an additional condition is set on u to get a uniform bound on $\|u\|_{L^2(\Omega)}$. We assume that $u \in L^\infty(\Omega)$, which is rather a non-restrictive and natural requirement in image processing since at every pixel the light intensity has finite energy. For instance, we introduce the condition $\|u\|_{L^\infty(\Omega)} \leq \|f\|_{L^\infty(\Omega)}$, which is reasonable in the context of image decomposition and in virtue of the smoothing properties of the functional.

We first give a result of existence of minimizers for the non-elliptic problem (4).

Theorem 7 (Existence of minimizers)**.** *Let us set* $X(\Omega) = \big\{u \in GSBV^2(\Omega) \cap L^\infty(\Omega) \text{ with } \|u\|_{L^\infty(\Omega)} \leq C_2\big\} \times H(div) \times \big\{Q \in W^{1,\infty}(\Omega) \mid \int_\Omega Q\,dx = 0\big\}$*, with* C_2 *a positive constant that depends only on* $\|f\|_{L^\infty(\Omega)}$*. Assuming* $\beta \leq \alpha \leq 2\beta$*,* $\gamma > 0$*,* $\mu > 0$ *and* $\beta > 0$*, there exists a minimizer* $(\bar{u}, \bar{\vec{g}}, \bar{Q}) \in X(\Omega)$ *of* $\bar{F}$*.*

Proof. The proof is based on an adaptation of arguments provided in [20]. □

We now give a Γ-convergence result.

Theorem 8 (Γ-convergence)**.** *Assume that* $\alpha = \beta$*,* $\kappa_\varepsilon > 0$ *with* $\kappa_\varepsilon = o(\varepsilon^4)$*,* $\xi_\varepsilon = \zeta_\varepsilon = 0$ *and* Ω *is strictly star-shaped. Then the family* $(\mathcal{F}_\varepsilon)$ Γ*-converges to* $\bar{F}$ *in the* $L^1(\Omega) \times H(div) \times W^{1,\infty}(\Omega) \times L^1(\Omega) \times L^1(\Omega)$ *topology (strong topology for* $L^1(\Omega)$ *and weak/weak-∗ topology for* $H(div)$ *and* $W^{1,\infty}(\Omega)$*) as* $\varepsilon \to 0^+$*. Besides, the limit point of* $(\bar{u}_\varepsilon, \bar{\vec{g}}_\varepsilon, \bar{Q}_\varepsilon, \bar{v}_{1,\varepsilon}, \bar{v}_{2,\varepsilon})$*, a pair of minimizers of* $\mathcal{F}_\varepsilon$*, when* ε *tends to* 0^+ *is of the form* $(\bar{u}, \bar{\vec{g}}, \bar{Q}, 1, 1)$ *with* $(\bar{u}, \bar{\vec{g}}, \bar{Q}) \in X(\Omega)$ *assuming* $\forall \varepsilon > 0$*,* $\|\bar{u}_\varepsilon\|_{L^\infty(\Omega)} \leq C_2$*. It means in particular that* $\lim_{\varepsilon \to 0^+} \big(\mathcal{F}_\varepsilon(\bar{u}_\varepsilon, \bar{\vec{g}}_\varepsilon, \bar{Q}_\varepsilon, \bar{v}_{1,\varepsilon}, \bar{v}_{2,\varepsilon}) - \bar{F}(\bar{u}, \bar{\vec{g}}, \bar{Q})\big) = 0.$

Proof. We refer the reader to [4][Theorem 3.1, 3.2 and 3.3] for some of the arguments that structure the proof. □

3. A nonlocal version of the modelling and its theoretical analysis

3.1. Motivations

Inspired by prior related works by Bourgain, Brezis and Mironescu [16] (—first concerned with the study of the limiting behavior of the norms of fractional Sobolev spaces $W^{s,p}$, $0 < s < 1$, $1 < p < \infty$ as $s \to 1$ and to a new characterization of the Sobolev spaces $W^{1,p}$, $1 < p < \infty$—), Aubert and Kornprobst [8] (—they question whether this characterization can be useful to solve variational problems—), Boulanger and co-authors [15] (—in which the authors address the question of the calculus of variations for nonlocal functionals—), Dávila [27], and Ponce [36] (—dedicated to expressing the semi-norms of first order Sobolev spaces and the BV space thanks to a nonlocal operator—), we introduce a sequence of radial mollifiers $\{\rho_n\}_{n\in\mathbb{N}}$ satisfying: $\forall n \in \mathbb{N}$, $\forall x \in \mathbb{R}$, $\rho_n(x) = \rho_n(|x|)$; $\forall n \in \mathbb{N}$, $\rho_n \geq 0$; $\forall n \in \mathbb{N}$, $\int_{\mathbb{R}} \rho_n(x)\,dx = 1$; $\forall \delta > 0$, $\lim_{n\to+\infty} \int_\delta^{+\infty} \rho_n(r)\,dr = 0$, and an associated sequence of functionals $\overline{\mathcal{F}_{\varepsilon,n}}$ depending on n and such that the component $\int_\Omega (v_2^2 + \kappa_\varepsilon)\,|\nabla^2 u|^2\,dx$ is approximated by an integral operator involving a differential quotient and the radial mollifier depicted above. It is shown that the approximated formulation admits minimizers for which regularity results are provided in a fractional Sobolev space. This theoretical study will lead to the derivation of a numerically tractable implementation, which is not the scope of the proposed work that focuses on the theoretical analysis.

This part is thus motivated by the idea of extending the concept of nonlocal gradients ([31]) to higher derivatives, of analyzing its theoretical properties and in particular, its convergence to classical second-order regularizers, and of deriving a nonlocal counterpart of the local model (5), with the underlying intention of devising a model numerically tractable and improving the overall quality of the local algorithm (by explaining second-order derivatives of u in terms of nonlocal quantities). Our model is also deeply inspired by [32] dedicated to a formulation of a nonlocal Hessian that combines the ideas of higher-order and nonlocal regularization for image restoration, and more largely to a novel characterization of higher Sobolev and BV-spaces. In this paper, the authors connect in particular the finiteness of $\liminf_{n\to\infty}\int_{\mathbb{R}^N}|\mathfrak{H}_n\,u(x)|^p\,dx$ (—$\mathfrak{H}_n\,u(x) := \frac{N(N+2)}{2}\int_{\mathbb{R}^N}\frac{u(x+h)-2u(x)+u(x-h)}{|h|^2}\frac{h\otimes h-\frac{|h|^2}{N+2}I_N}{|h|^2}\,\rho_n(h)\,dh$—) with the inclusion of $u\in L^p(\mathbb{R}^N)$, $1<p<\infty$, in $W^{2,p}(\mathbb{R}^N)$. They thus introduce a nonlocal Hessian that is derivative free, only requiring the considered function u to belong to an L^p-space. As in [32], our model is derivative free, involving a built-in symmetry that associates triples of points; the main difference lies in the independent treatment of the directional derivatives, yielding a nonlocal version not of $\int_{\mathbb{R}^2}|\nabla^2 u|^2\,dx$, but of $\int_{\mathbb{R}^2}\left(\frac{\partial^2 u}{\partial x_1^2}\right)^2+\left(\frac{\partial^2 u}{\partial x_2^2}\right)^2\,dx$ ($x=(x_1,x_2)\in\mathbb{R}^2$), thus removing the control of the L^2-norm of $\frac{\partial^2 u}{\partial x_1\partial x_2}$. We will show nevertheless with the theory of tempered distributions that if u, $\frac{\partial^2 u}{\partial x_1^2}$, $\frac{\partial^2 u}{\partial x_2^2}\in L^2(\mathbb{R}^2)$, then $u\in W^{2,2}(\mathbb{R}^2)$. This modelling inherits fine analytical properties, has the advantage of being numerically more tractable compared to [32], particularly in the derivation of the Euler-Lagrange equation satisfied by u, and is straightforwardly connected to our imaging problem, which is not the case in [32].

At last, for the sake of completeness, we refer the interested reader to other papers dealing with higher-order regularizations: [23] (—in which the authors propose higher-order models by means of an infimal convolution of two convex regularizers—), [24] (—in which a weighted version of the Laplacian is provided—), [25] (—introducing the Euler-elastica functional), [17] (—proposing the total generalized variation—), or [11] (—bounded Hessian regularization—).

3.2. Notations and preliminary results

Let (e_1,e_2) be the canonical basis of $\mathbb{R}^2$. We use dx ($x=(x_1,x_2)$) for integration with respect to the Lebesgue measure on $\mathbb{R}^2$ and dt, ds, dh for various integrations with respect to the Lebesgue measure on $\mathbb{R}$. The differentiation indices will be a pair $\alpha=(\alpha_1,\alpha_2)$, where α_i is the order of the partial derivative in the variable x_i, and the total order of the derivative is denoted by $|\alpha|=\alpha_1+\alpha_2$. We will use the shortened notation $D^\alpha u=\frac{\partial^{|\alpha|}u}{\partial {x_1}^{\alpha_1}\partial {x_2}^{\alpha_2}}$.

Several functional spaces are required (see [28] for instance): $\mathcal{C}_c^\infty(\mathbb{R}^2)$ (or $\mathcal{D}(\mathbb{R}^2)$), the space of $\mathcal{C}^\infty(\mathbb{R}^2)$ functions with compact support in $\mathbb{R}^2$. Given an integer $j \geq 0$, we define the family of spaces $\mathcal{C}_b^j(\mathbb{R}^2)$ ([28, Definition 2.2.1, p. 69]) by setting

$$\mathcal{C}_b^j(\mathbb{R}^2) = \left\{u \in \mathcal{C}^j(\mathbb{R}^2) \,|\, \forall \alpha \in \mathbb{N}^2,\, |\alpha| \leq j,\, \exists K_\alpha,\, \|D^\alpha u\|_\infty \leq K_\alpha\right\}.$$

For a positive real number λ, the subspace $\mathcal{C}_b^{j,\lambda}(\mathbb{R}^2)$ consists of the functions in $\mathcal{C}_b^j(\mathbb{R}^2)$ such that if $|\alpha| \leq j$, then

$$\exists C_{\alpha,\lambda},\, \forall x, y \in \mathbb{R}^2,\, |D^\alpha u(x) - D^\alpha u(y)| \leq C_{\alpha,\lambda}\, |x-y|^\lambda.$$

For $m \in \mathbb{N}$ and $1 \leq p \leq \infty$ and Ω being an open subset of $\mathbb{R}^2$, we define the Sobolev space $W^{m,p}(\Omega)$ ([28, Definition 2.1, p. 57]) as

$$W^{m,p}(\Omega) = \left\{u \in L^p(\Omega) \,|\, \forall \alpha \in \mathbb{N}^2,\, |\alpha| \leq m \Rightarrow D^\alpha u \in L^p(\Omega)\right\}.$$

We denote by $\mathcal{S}(\mathbb{R}^2)$ ([28, Definition 4.1, p. 179]) the set of rapidly decreasing functions in $\mathbb{R}^2$: a function φ is said to be rapidly decreasing in $\mathbb{R}^2$ if $\varphi \in \mathcal{C}^\infty(\mathbb{R}^2)$ and if

$$\forall j \in \mathbb{N}^2,\, \forall k \in \mathbb{N},\, |x|^k\, D^j\varphi \in L^\infty(\mathbb{R}^2).$$

We let $\mathcal{S}'(\mathbb{R}^2)$ denote the topological dual of $\mathcal{S}(\mathbb{R}^2)$, set of tempered distributions.

Let now $s > 0$ be a real number. We let ([28, Definition 4.7, p. 181])

$$H^s(\mathbb{R}^2) = \left\{u \in L^2(\mathbb{R}^2) \,|\, \left\{\xi \mapsto (1+|\xi|^2)^{s/2}\mathcal{F}(u)(\xi)\right\} \in L^2(\mathbb{R}^2)\right\},$$

$\mathcal{F}$, denoting the Fourier transform. If $s = m \in \mathbb{N}$, then the space $H^s(\mathbb{R}^2)$ coincides with the classical Sobolev space $W^{m,2}(\mathbb{R}^2)$. If $s \in \mathbb{R}\setminus\mathbb{N}$ with $s \geq 1$, then the space $H^s(\mathbb{R}^2)$ coincides with the fractional Sobolev space $W^{s,2}(\mathbb{R}^2)$ ([28, Definition 4.56, p. 219]) defined by

$$W^{s,2}(\mathbb{R}^2) = \left\{u \in W^{[s],2}(\mathbb{R}^2) \,|\, D^j u \in W^{s-[s],p}(\mathbb{R}^2),\, \forall \vec{j},\, |\vec{j}| = [s]\right\},$$

$[\cdot]$ denoting the integer part, and when $\sigma \in (0,1)$ ([28, Definition 4.23, p. 192]),

$$W^{\sigma,2}(\mathbb{R}^2) = \left\{u \in L^2(\mathbb{R}^2) \,|\, \int_{\mathbb{R}^2}\int_{\mathbb{R}^2} \frac{|u(x)-u(y)|^2}{|x-y|^{2\sigma+2}}\, dx\, dy < \infty\right\}.$$

At last, the properties of the considered kernel ρ_n are those depicted above, and we will use several times the following generalized result of Spector ([38, p. 58]):

Lemma 1. *If $E \subset \mathbb{R}$ is bounded and measurable, then $\forall p \in \mathbb{N}^*$,*

$$\lim_{n\to+\infty} \int_E |x|^p \, \rho_n(x)\, dx = 0. \tag{6}$$

Proof. Fixing $\delta > 0$,

$$\begin{aligned}\limsup_{n\to+\infty} \int_E |x|^p \, \rho_n(x)\, dx \leq & \limsup_{n\to+\infty} \int_{\{|x|>\delta\}\cap E} |x|^p \, \rho_n(x)\, dx \\ & + \limsup_{n\to+\infty} \int_{\{|x|\leq\delta\}} |x|^p \, \rho_n(x)\, dx, \\ \leq & C_{\delta,E,p} \lim_{n\to+\infty} \int_{|x|>\delta} \rho_n(x)\, dx + \delta^p.\end{aligned}$$

The result follows from the properties of ρ_n and by sending δ to 0. □

Equipped with this material, we now propose a derivative free nonlocal formulation of the L^2-norms $\int_{\mathbb{R}^2} |D^{(2,0)}u|^2\, dx$ and $\int_{\mathbb{R}^2} |D^{(0,2)}u|^2\, dx$ respectively. We start off with the definition of such a nonlocal version for smooth functions.

Theorem 9. *Let $u \in \mathcal{C}_c^4(\mathbb{R}^2)$. Then*

$$\int_{\mathbb{R}^2}\int_{\mathbb{R}} \frac{|u(x+he_i) - 2u(x) + u(x-he_i)|^2}{|h|^4} \rho_n(h)\, dh\, dx \underset{n\to+\infty}{\longrightarrow} \begin{cases} \int_{\mathbb{R}^2} |D^{(2,0)}u|^2\, dx & \text{if } i=1 \\ \int_{\mathbb{R}^2} |D^{(0,2)}u|^2\, dx & \text{if } i=2 \end{cases}.$$

Proof. We deal with the case $i = 1$.

Let us define $H_1u(x) := \int_{\mathbb{R}} \frac{|u(x+he_1) - 2u(x) + u(x-he_1)|^2}{|h|^4} \rho_n(h)\, dh.$ Let $R > 0$ be fixed.

$$\begin{aligned}H_1u(x) = & \int_{\{|h|\leq R\}} \frac{|u(x+he_1) - 2u(x) + u(x-he_1)|^2}{|h|^4} \rho_n(h)\, dh \\ & + \int_{\{|h|>R\}} \frac{|u(x+he_1) - 2u(x) + u(x-he_1)|^2}{|h|^4} \rho_n(h)\, dh.\end{aligned}$$

But $u(x+he_1)-2u(x)+u(x-he_1) = h^2 \int_0^1 \int_0^1 D^{(2,0)}u(x+h(s+t-1)e_1)\,dt\,ds$ and from Taylor's expansion $\frac{u(x+he_1)-2u(x)+u(x-he_1)}{h^2} = D^{(2,0)}u(x) + \frac{h^2}{12}\,D^{(4,0)}$ $u(\zeta_{x_1,h}, x_2)$, so that

$$\begin{aligned}&\int_{\{|h|>R\}} \left[\int_0^1 \int_0^1 D^{(2,0)}u(x+h(s+t-1)e_1)\,dt\,ds\right]^2 \rho_n(h)\,dh\\&\leq \|D^{(2,0)}u\|^2_{L^\infty(\mathbb{R}^2)} \int_{\{|h|>R\}} \rho_n(h)\,dh \underset{n\to+\infty}{\longrightarrow} 0.\end{aligned}$$

Using the previous Taylor's expansion, the properties of ρ_n and lemma 1 yields

$$\int_{\{|h|\leq R\}} \frac{|u(x+he_1)-2u(x)+u(x-he_1)|^2}{|h|^4}\,\rho_n(h)\,dh \underset{n\to+\infty}{\longrightarrow} |D^{(2,0)}u(x)|^2$$

and therefore $H_1u(x)$ converges to $|D^{(2,0)}u(x)|^2$ everywhere. We now aim to prove that $\int_{\mathbb{R}^2} |H_1u(x) - |D^{(2,0)}u(x)|^2|\,dx \underset{n\to+\infty}{\longrightarrow} 0$. We assume without loss of generality that $\operatorname{supp} u \subset B(0,R)$. We first show that $\forall\epsilon>0$, $\exists L = L(\epsilon) > 1$ such that

$$\sup_n \int_{B(0,LR)^c} |H_1u(x)|\,dx \leq \epsilon.$$

One has, making a change of variable,

$$\begin{aligned}&\int_{B(0,LR)^c} |H_1u(x)|\,dx\\&= \int_{B(0,LR)^c} \int_{\mathbb{R}} \frac{|u(x+he_1)+u(x-he_1)|^2}{|h|^4}\,\rho_n(h)\,dh\,dx,\\&\leq 2\int_{B(0,LR)^c} \int_{\mathbb{R}} \frac{|u(x+he_1)|^2+|u(x-he_1)|^2}{|h|^4}\,\rho_n(h)\,dh\,dx,\\&\leq 4\int_{B(0,LR)^c} \int_{\{h\,|\,x+he_1\in B(0,R)\}} \frac{|u(x+he_1)|^2}{|h|^4}\,\rho_n(h)\,dh\,dx,\\&\leq \frac{4}{(L-1)^4R^4} \int_{B(0,LR)^c} \int_{\{h\,|\,x+he_1\in B(0,R)\}} |u(x+he_1)|^2\,\rho_n(h)\,dh\,dx,\\&\leq \frac{4}{(L-1)^4R^4}\,\|u\|^2_{L^2(\mathbb{R}^2)}\,\|\rho_n\|_{L^1(\mathbb{R})} = \frac{4}{(L-1)^4R^4}\,\|u\|^2_{L^2(\mathbb{R}^2)}.\end{aligned}$$

Thus $\forall \epsilon > 0$, $\exists L = L(\epsilon) > 1$, $\forall n \in \mathbb{N}$, $\int_{B(0,LR)^c} |H_1 u(x)|\, dx \le \epsilon$, which means

$$\sup_{n\in\mathbb{N}} \int_{B(0,LR)^c} |H_1 u(x)|\, dx \le \epsilon.$$

As

$$\int_{\mathbb{R}^2} |H_1 u(x) - |D^{(2,0)}u(x)|^2|\, dx = \int_{B(0,LR)} |H_1 u(x) - |D^{(2,0)}u(x)|^2|\, dx + \int_{B(0,LR)^c} |H_1 u(x)|\, dx,$$

$$\limsup_{n\to+\infty} \int_{\mathbb{R}^2} |H_1 u(x) - |D^{(2,0)}u(x)|^2|\, dx \le \limsup_{n\to+\infty} \int_{B(0,LR)} |H_1 u(x) - |D^{(2,0)}u(x)|^2|\, dx + \epsilon.$$

Now, $H_1 u$ converges pointwise to $|D^{(2,0)}u(x)|^2$ and on $B(0,LR)$, $H_1 u(x) \le \|D^{(2,0)}u\|^2_{L^\infty(\mathbb{R}^2)}$, which is integrable on $B(0,LR)$. It follows from the dominated convergence theorem that

$$\int_{B(0,LR)} |H_1 u(x) - |D^{(2,0)}u(x)|^2|\, dx \underset{n\to+\infty}{\longrightarrow} 0,$$

yielding

$$\limsup_{n\to+\infty} \int_{\mathbb{R}^2} |H_1 u(x) - |D^{(2,0)}u(x)|^2|\, dx \le \epsilon,$$

and in the end,

$$\lim_{n\to+\infty} \int_{\mathbb{R}^2} |H_1 u(x) - |D^{(2,0)}u(x)|^2|\, dx = 0. \qquad \square$$

In fact, we have an analogous convergence result for $u \in W^{2,2}(\mathbb{R}^2)$ that we establish with the following lemma.

Lemma 2. *Suppose that* $u \in W^{2,2}(\mathbb{R}^2)$. *Then* $\int_{\mathbb{R}^2}\int_{\mathbb{R}} \frac{|u(x+he_i)-2u(x)+u(x-he_i)|^2}{|h|^4} \rho_n(h)\, dh\, dx$ *is well-defined and*

$$\int_{\mathbb{R}^2}\int_{\mathbb{R}} \frac{|u(x+he_i)-2u(x)+u(x-he_i)|^2}{|h|^4} \rho_n(h)\, dh\, dx \le \begin{cases} \|D^{(2,0)}u\|^2_{L^2(\mathbb{R}^2)} & \text{if } i=1 \\ \|D^{(0,2)}u\|^2_{L^2(\mathbb{R}^2)} & \text{if } i=2 \end{cases}.$$

Proof. We focus on the case $i = 1$.

Let us begin by estimates for a function $u \in \mathcal{C}^\infty(\mathbb{R}^2) \cap W^{2,2}(\mathbb{R}^2)$. Using Fubini-Tonelli's theorem and Jensen's inequality,

$$\begin{aligned}
&\int_{\mathbb{R}^2} \int_{\mathbb{R}} \frac{|u(x+he_1) - 2u(x) + u(x-he_1)|^2}{|h|^4} \rho_n(h)\, dh\, dx \\
&\leq \int_{\mathbb{R}^2} \int_{\mathbb{R}} \left[\int_0^1 \int_0^1 |D^{(2,0)} u(x + (t+s-1)he_1)|^2\, ds\, dt \right] \rho_n(h)\, dh\, dx, \\
&\leq \|D^{(2,0)} u\|^2_{L^2(\mathbb{R}^2)}.
\end{aligned}$$

Consider now a sequence $(u_k)_{k\in\mathbb{N}}$ in $\mathcal{C}^\infty(\mathbb{R}^2) \cap W^{2,2}(\mathbb{R}^2)$ approximating u in $W^{2,2}(\mathbb{R}^2)$ (see [28, Proposition 2.12, p. 60] for a density result). From the above,

$$\int_{\mathbb{R}^2} \int_{\mathbb{R}} \frac{|u_k(x+he_1) - 2u_k(x) + u_k(x-he_1)|^2}{|h|^4} \rho_n(h)\, dh\, dx \leq \|D^{(2,0)} u_k\|^2_{L^2(\mathbb{R}^2)}.$$

As $(u_k)_{k\in\mathbb{N}}$ converges to u in $W^{2,2}(\mathbb{R}^2) \circlearrowleft \mathcal{C}_b^{0,\lambda}(\mathbb{R}^2)$ for every $\lambda < 1$ ([28, Theorem 2.31, p. 69]), $(u_k)_{k\in\mathbb{N}}$ uniformly converges to u, so pointwise everywhere. Fatou's lemma allows us to conclude that

$$\begin{aligned}
&\int_{\mathbb{R}} \frac{|u(x+he_1) - 2u(x) + u(x-he_1)|^2}{|h|^4} \rho_n(h)\, dh \\
&\leq \liminf_{k\to+\infty} \int_{\mathbb{R}} \frac{|u_k(x+he_1) - 2u_k(x) + u_k(x-he_1)|^2}{|h|^4} \rho_n(h)\, dh,
\end{aligned}$$

and

$$\begin{aligned}
&\int_{\mathbb{R}^2} \int_{\mathbb{R}} \frac{|u(x+he_1) - 2u(x) + u(x-he_1)|^2}{|h|^4} \rho_n(h)\, dh\, dx \\
&\leq \int_{\mathbb{R}^2} \liminf_{k\to+\infty} \int_{\mathbb{R}} \frac{|u_k(x+he_1) - 2u_k(x) + u_k(x-he_1)|^2}{|h|^4} \rho_n(h)\, dh\, dx.
\end{aligned}$$

Setting $F_k(x) := \int_{\mathbb{R}} \frac{|u_k(x+he_1) - 2u_k(x) + u_k(x-he_1)|^2}{|h|^4} \rho_n(h)\, dh$, $(F_k)_{k\in\mathbb{N}}$ is a sequence of functions of $L^1(\mathbb{R}^2)$ such that $\sup_k \int_{\mathbb{R}^2} F_k < \infty$, so applying Fatou's lemma a second time yields

$$\int_{\mathbb{R}^2} \int_{\mathbb{R}} \frac{|u(x+he_1) - 2u(x) + u(x-he_1)|^2}{|h|^4} \rho_n(h)\, dh\, dx$$

$$\leq \liminf_{k\to+\infty} \int_{\mathbb{R}^2}\int_{\mathbb{R}} \frac{|u_k(x+he_1)-2u_k(x)+u_k(x-he_1)|^2}{|h|^4}\rho_n(h)\,dh\,dx,$$
$$\leq \liminf_{k\to+\infty} \|D^{(2,0)}u_k\|^2_{L^2(\mathbb{R}^2)} = \|D^{(2,0)}u\|^2_{L^2(\mathbb{R}^2)}. \qquad \square$$

With this preliminary lemma, we now state the main result.

Theorem 10. *Let $u \in W^{2,2}(\mathbb{R}^2)$. Then*

$$\int_{\mathbb{R}^2}\int_{\mathbb{R}} \frac{|u(x+he_i)-2u(x)+u(x-he_i)|^2}{|h|^4}\rho_n(h)\,dh\,dx$$
$$\underset{n\to+\infty}{\longrightarrow} \begin{cases} \|D^{(2,0)}u\|^2_{L^2(\mathbb{R}^2)} & \text{if } i=1,\\ \|D^{(0,2)}u\|^2_{L^2(\mathbb{R}^2)} & \text{if } i=2 \end{cases}.$$

Proof. We restrict ourselves to the case $i=1$.

Let $\epsilon>0$. By density, there exists $v_\epsilon \in \mathcal{C}^\infty_c(\mathbb{R}^2)$ such that

$$\|D^{(2,0)}u - D^{(2,0)}v_\epsilon\|_{L^2(\mathbb{R}^2)} \leq \epsilon.$$

Let us set $u_n(x,h) = \frac{u(x+he_1)-2u(x)+u(x-he_1)}{h^2}\,\rho_n^{\frac12}(h)$. $u_n \in L^2(\mathbb{R}^2\times\mathbb{R})$ and $\|u_n\|_{L^2(\mathbb{R}^2\times\mathbb{R})} \leq \|D^{(2,0)}u\|_{L^2(\mathbb{R}^2)}$. Denoting by $v_{n,\epsilon} := \frac{v_\epsilon(x+he_1)-2v_\epsilon(x)+v_\epsilon(x-he_1)}{h^2}\,\rho_n^{\frac12}(h)$, we thus have

$$\|u_n - v_{n,\epsilon}\|_{L^2(\mathbb{R}^2\times\mathbb{R})} \leq \|D^{(2,0)}u - D^{(2,0)}v_\epsilon\|_{L^2(\mathbb{R}^2)} \leq \epsilon,$$

and from the second triangle inequality,

$$|\|u_n\|_{L^2(\mathbb{R}^2\times\mathbb{R})} - \|v_{n,\epsilon}\|_{L^2(\mathbb{R}^2\times\mathbb{R})}| \leq \epsilon.$$

To conclude,

$$\begin{aligned}\Big|\|u_n\|_{L^2(\mathbb{R}^2\times\mathbb{R})} - \|D^{(2,0)}u\|_{L^2(\mathbb{R}^2)}\Big| &\leq \big|\|u_n\|_{L^2(\mathbb{R}^2\times\mathbb{R})} - \|v_{n,\epsilon}\|_{L^2(\mathbb{R}^2\times\mathbb{R})}\big| \\ &+ \Big|\|v_{n,\epsilon}\|_{L^2(\mathbb{R}^2\times\mathbb{R})} - \|D^{(2,0)}v_\epsilon\|_{L^2(\mathbb{R}^2)}\Big| \\ &+ \Big|\|D^{(2,0)}v_\epsilon\|_{L^2(\mathbb{R}^2)} - \|D^{(2,0)}u\|_{L^2(\mathbb{R}^2)}\Big|, \\ &\leq 2\epsilon + \Big|\|v_{n,\epsilon}\|_{L^2(\mathbb{R}^2\times\mathbb{R})} - \|D^{(2,0)}v_\epsilon\|_{L^2(\mathbb{R}^2)}\Big|.\end{aligned}$$

It leads to $\limsup_{n\to+\infty} \big|\|u_n\|_{L^2(\mathbb{R}^2\times\mathbb{R})} - \|D^{(2,0)}u\|_{L^2(\mathbb{R}^2)}\big| \leq 2\epsilon$ and then $\|u_n\|_{L^2(\mathbb{R}^2\times\mathbb{R})} \underset{n\to+\infty}{\longrightarrow} \|D^{(2,0)}u\|_{L^2(\mathbb{R}^2)}$. $\square$

Equipped with these theoretical results and characterization, we reformulate our local problem into a nonlocal form.

3.3. Connection to the local imaging problem

Due to the independent treatment of the directional derivatives in the previous nonlocal formulations, we slightly modify the local problem into

$$\begin{aligned}\inf \overline{\mathcal{F}_\varepsilon}(u,\vec{g},Q,v_1,v_2) = \; & \|f-u-\operatorname{div}\vec{g}\|^2_{L^2(\Omega)} + \mu \,\||\nabla Q|\|_{L^\infty(\Omega)} \\ & + \frac{\gamma}{2}\,\||\vec{g}-\nabla Q|\|^2_{L^2(\Omega)} \\ & + \rho \int_\Omega (v_2^2+\kappa_\varepsilon)\,\left(|D^{(2,0)}u|^2+|D^{(0,2)}u|^2\right)\,dx \\ & + \xi_\varepsilon \int_\Omega (v_1^2+\zeta_\epsilon)\,|\nabla u|^2\,dx + (\alpha-\beta)\,\mathcal{G}_\varepsilon(v_1) + \beta\,\mathcal{G}_\varepsilon(v_2). \end{aligned} \tag{7}$$

While the functional spaces for Q, $\vec{g}$, and v_1 are unchanged, the unknowns u and v_2 are now searched in the functional spaces $W_0^{1,2}(\Omega)\cap W^{2,2}(\Omega)$ and $\left\{v_2 \in W^{1,2}(\Omega,[0,1]) \,|\, \gamma_0\, v_2 = 1\right\}$ respectively, γ_0 denoting the trace operator. The reasons for such requirements will be made clearer in the following. Nevertheless, these assumptions are reasonable and not restrictive if we assume for instance that the observed image f is with compact support. Existence of minimizers is still guaranteed as stated below.

Theorem 11. *Let Ω be a regular bounded open subset of $\mathbb{R}^2$. With $\kappa_\varepsilon,\xi_\varepsilon,\zeta_\varepsilon>0$, problem (7) admits minimizers ($\overline{u}=\overline{u_\varepsilon},\overline{\vec{g}}=\overline{\vec{g}_\varepsilon},\overline{Q}=\overline{Q_\varepsilon},\overline{v_1}=\overline{v_{1,\varepsilon}},\overline{v_2}=\overline{v_{2,\varepsilon}}$) on $W_0^{1,2}(\Omega)\cap W^{2,2}(\Omega)\times H(div)\times\left\{Q\in W^{1,\infty}(\Omega)\,|\,\int_\Omega Q\,dx=0\right\}\times W^{1,2}(\Omega,[0,1])\times\left\{v_2\in W^{1,2}(\Omega,[0,1])\,|\,\gamma_0 v_2=1\right\}$.*

Proof. The proof rests upon two major facts: (i) the space $W_0^{1,2}(\Omega)$ is a strongly closed convex subspace of $W^{1,2}(\Omega)$ by continuity of the trace map, so according to [18, Theorem III.7, p. 38], it is a weakly closed convex subspace. (ii) the mapping $\widehat{\|\cdot\|}: u\mapsto\left(\|D^{(2,0)}u\|^2_{L^2(\Omega)}+\|D^{(0,2)}u\|^2_{L^2(\Omega)}\right)^{\frac{1}{2}}$ is a norm on $W_0^{1,2}(\Omega)\cap W^{2,2}(\Omega)$ equivalent to the usual norm on $W^{2,2}(\Omega)$ that we denote by $\|\cdot\|_{2,\Omega}$. The homogeneity axiom as well as the triangle inequality are straightforwardly obtained. Let $u\in W_0^{1,2}(\Omega)\cap W^{2,2}(\Omega)$ be such that $\widehat{\|u\|}=0$. Then from Green's formula, $\int_\Omega|\nabla u|^2\,dx=0$ and from Poincaré's inequality, $u=0$ almost everywhere on Ω.

Now let us denote by $\mathcal{A}$ the mapping $\mathcal{A}: W_0^{1,2}(\Omega)\cap W^{2,2}(\Omega)\to L^2(\Omega)$ such that $\forall u\in W_0^{1,2}(\Omega)\cap W^{2,2}(\Omega)$, $\mathcal{A}(u)=\Delta u$. For every $f\in L^2(\Omega)$, let us introduce the unique solution (Lax-Milgram theorem) $u \in W_0^{1,2}(\Omega)$ of the variational problem: $\forall v \in W_0^{1,2}(\Omega)$,

$$\int_\Omega \langle \nabla u, \nabla v\rangle_{\mathbb{R}^2}\, dx = -\int_\Omega f\, v\, dx.$$

As the boundary of Ω is sufficiently smooth, a regularity result (see [18, Section IX.6, p. 181] for instance) gives that $u \in W^{2,2}(\Omega)$. As $\Delta u = f$, it follows that $\mathcal{A}$ (which is a continuous mapping since $\|\Delta u\|_{L^2(\Omega)} \leq \sqrt{2}\,\|u\|_{2,\Omega}$) is a bijection from $W_0^{1,2}(\Omega) \cap W^{2,2}(\Omega)$ to $L^2(\Omega)$. The bounded inverse theorem enables us to conclude that the inverse mapping is continuous as well, implying the existence of a constant $C > 0$ such that $\forall u \in W_0^{1,2}(\Omega) \cap W^{2,2}(\Omega)$, $\|u\|_{2,\Omega} \leq C\,\|\Delta u\|_{L^2(\Omega)} \leq \sqrt{2}C\,\widehat{\|u\|}$. □

Our mathematical material being formulated on $\mathbb{R}^2$ rather than Ω, in our nonlocal model, we propose searching for u in a subspace of $W_0^{1,2}(\Omega)$ and for v_2 in $W^{1,2}(\Omega, [0,1])$ such that $\gamma_0\, v_2 = 1$.

Theorem 12. *Let Ω be a regular bounded open subset of $\mathbb{R}^2$ with boundary of class $\mathcal{C}^2$. Let us assume that the functions $t \mapsto \rho_n(t)$, $t \mapsto t^q \rho_n(t)$ are non-increasing for $t \geq 0$ and $q \in]0,1[$. (Such a function ρ_n exists: for instance, with $q \in]0,1[$, $\rho(t) = \frac{e^{-|t|}}{|t|^q}$ and $\rho_n(t) = C\, n\, \rho(nt)$ with $C = \frac{1}{\int_{\mathbb{R}} \rho(t)\, dt}$). With $\kappa_\varepsilon, \xi_\varepsilon, \zeta_\varepsilon > 0$, for any $n \in \mathbb{N}^*$, problem*

$$\begin{aligned}\inf \overline{\mathcal{F}_{\varepsilon,n}}(u, \vec{g}, Q, v_1, v_2) =\ & \|f - u - div\, \vec{g}\|^2_{L^2(\Omega)} + \mu\, \||\nabla Q|\|_{L^\infty(\Omega)} \\ & + \rho \int_{\mathbb{R}^2} (v_{2,e}^2(x) + \kappa_\varepsilon) \sum_{i=1}^2 \int_{\mathbb{R}} \frac{|u_e(x + he_i) - 2u_e(x) + u_e(x - he_i)|^2}{|h|^4} \rho_n(h)\, dh \\ & + \frac{\gamma}{2}\, \||\vec{g} - \nabla Q|\|^2_{L^2(\Omega)} + \xi_\varepsilon \int_\Omega (v_1^2 + \zeta_\epsilon)\, |\nabla u|^2\, dx + (\alpha - \beta)\, \mathcal{G}_\varepsilon(v_1) + \beta\, \mathcal{G}_\varepsilon(v_2),\end{aligned} \tag{8}$$

where $v_{2,e}$ and u_e are respectively the extensions of v_2 according to [18, Theorem IX.7, p. 158] —by construction, $0 \leq v_{2,e} \leq 1$ a.e.—and of u on $\mathbb{R}^2$ by 0 (—with the regularity assumed on Ω, $v_{2,e}$ and $u_{2,e}$ are in $W^{1,2}(\mathbb{R}^2)$—), admits minimizers $(\overline{u_n} = \overline{u_{\varepsilon,n}}, \overline{\vec{g_n}} = \overline{\vec{g_{\varepsilon,n}}}, \overline{Q_n} = \overline{Q_{\varepsilon,n}}, \overline{v_{1,n}} = \overline{v_{1,\varepsilon,n}}, \overline{v_{2,n}} = \overline{v_{2,\varepsilon,n}})$ on $W_0^{1,2}(\Omega) \cap W^{s,2}(\Omega) \times H(div) \times \left\{Q \in W^{1,\infty}(\Omega) \,|\, \int_\Omega Q\, dx = 0\right\} \times W^{1,2}(\Omega, [0,1]) \times \left\{v_2 \in W^{1,2}(\Omega, [0,1]) \,|\, \gamma_0 v_2 = 1\right\}$, with $s \in \left[\frac{3}{2}, 2\right[$.

Proof. The functional is proper, take $v_1 \equiv 1$, $v_2 \equiv 1$, $\vec{g} \equiv \vec{0}$, $Q \equiv 0$, and $u \equiv 0$, since f is assumed to be sufficiently smooth (i.e. at least $L^2(\Omega)$) on Ω which is bounded. Let us now consider a minimizing sequence $(u_n^l, \vec{g_n}^l, Q_n^l, v_{1,n}^l, v_{2,n}^l)$ on $W_0^{1,2}(\Omega)\times H(div) \times \left\{Q \in W^{1,\infty}(\Omega) \mid \int_\Omega Q\,dx = 0\right\}$ $\times W^{1,2}(\Omega,[0,1]) \times \left\{v_2 \in W^{1,2}(\Omega,[0,1]) \mid \gamma_0\, v_2 = 1\right\}$ (the dependency on ε is not explicitly mentionned here for compactness). We will show that in fact, $u_n^l \in W_0^{1,2}(\Omega) \cap W^{s,2}(\Omega)$.

1. **Extraction of convergent subsequences**:

   - $\overline{\mathcal{F}_{\varepsilon,n}}(u_n^l, \vec{g_n}^l, Q_n^l, v_{1,n}^l, v_{2,n}^l) \geq \mu\, \||\nabla Q_n^l|\|_{L^\infty(\Omega)}$. As $\int_\Omega Q_n^l\,dx = 0$ for all $l \in \mathbb{N}$, we can use Poincaré-Wirtinger inequality, which leads us to the existence of a subsequence of Q_n^l still denoted by Q_n^l weakly-$*$ converging to $\overline{Q_n}$ in $W^{1,\infty}(\Omega)$. As the weak-$*$ convergence in $W^{1,\infty}(\Omega)$ implies uniform convergence, $\int_\Omega \overline{Q_n}(x)\,dx = 0$.

   - $\overline{\mathcal{F}_{\varepsilon,n}}(u_n^l, \vec{g_n}^l, Q_n^l, v_{1,n}^l, v_{2,n}^l) \geq (\alpha - \beta)\varepsilon \|\nabla v_{1,n}^l\|^2_{L^2(\Omega)}$. By noticing that $v_{1,n}^l \in L^\infty(\Omega)$ with $0 \leq v_{1,n}^l \leq 1$ a.e., $\int_\Omega v_{1,n}^l\,dx \leq 1$ and Poincaré-Wirtinger inequality gives us the existence of a subsequence of $v_{1,n}^l$ still denoted by $v_{1,n}^l$ weakly converging to $\overline{v_{1,n}}$ in $W^{1,2}(\Omega)$. Since $W^{1,2}(\Omega) \underset{c}{\circlearrowleft} L^2(\Omega)$, $v_{1,n}^l$ strongly converges to $\overline{v_{1,n}}$ in $L^2(\Omega)$ and so pointwise almost everywhere up to a subsequence. We deduce that $\overline{v_{1,n}} \in W^{1,2}(\Omega,[0,1])$.

   - In the same way, we have $v_{2,n}^l$ weakly converging to $\overline{v_{2,n}}$ in $W^{1,2}(\Omega)$ with $\overline{v_{2,n}} \in W^{1,2}(\Omega,[0,1])$ and $\gamma_0\,\overline{v_{2,n}} = 1$ by continuity of the trace operator.

   - $\overline{\mathcal{F}_{\varepsilon,n}}(u_n^l, \vec{g_n}^l, Q_n^l, v_{1,n}^l, v_{2,n}^l) \geq \xi_\varepsilon \zeta_\varepsilon \|\nabla u_n^l\|^2_{L^2(\Omega)}$. By Poincaré inequality and the continuity of the trace operator, we get the existence of a subsequence of u_n^l still denoted by u_n^l weakly converging to $\overline{u_n} \in W_0^{1,2}(\Omega)$ in $W^{1,2}(\Omega)$.

     Let us set $E_n^l(h) = \int_{\mathbb{R}^2} |u_{n,e}^l(x+he_1) - 2u_{n,e}^l(x) + u_{n,e}(x-he_1)|^2\,dx$ where $u_{n,e}^l$ denotes the extension by 0 of u_n^l on $\mathbb{R}^2$. Here again, due to the assumption on Ω, $u_{n,e}^l$ belongs to $W^{1,2}(\mathbb{R}^2)$. One can prove that $E_n^l(2h) \leq 16 E_n^l(h)$. By using Fubini-Tonelli theorem, we have $\int_{\mathbb{R}^2}\int_{\mathbb{R}} \frac{|u_{n,e}^l(x+he_1) - 2u_{n,e}^l(x) + u_{n,e}^l(x-he_1)|^2}{|h|^4}\rho_n(h)\,dh\,dx = \int_{\mathbb{R}} \frac{E_n^l(h)}{|h|^4}\rho_n(h)\,dh = 2\int_0^\infty \frac{E_n^l(h)}{|h|^4}\rho_n(h)\,dh \leq \overline{\mathcal{F}_{\varepsilon,n}}(u_n^l, \vec{g}_n^l, Q_n^l, v_{1,n}^l, v_{2,n}^l)$. We then apply [8, Lemma 3.2] by taking $M = \delta = 1$,

$g(t) = \dfrac{E_n^l(t)}{t^{q+1}}$, $k(t) = t^{q-3}\rho_n(t)$ and we get:

$$\int_0^1 \frac{E_n^l(h)}{|h|^4}\rho_n(h)\,dh \geq C(1)\int_0^1 \frac{E_n^l(t)}{|t|^{q+1}}\,dt \int_0^1 t^{q-3}\rho_n(t)\,dt.$$

(We will see further that the condition of monotonicity on k is fulfilled). We now need g to verify the assumption of this lemma, that is to say, $g(\frac{t}{2}) \geq g(t)$. We know that $g(\frac{t}{2}) = \dfrac{E_n^l(\frac{t}{2})2^{q+1}}{t^{q+1}} \geq 2^{q-3}g(t)$. Thus if $q \geq 3$, this condition is fulfilled. By using the properties of ρ_n, we deduce first that $\int_0^1 \dfrac{E_n^l(t)}{|t|^{q+1}}\,dt \leq C$ with C independant of l. Then $\int_1^\infty \dfrac{E_n^l(t)}{|t|^{q+1}}\,dt \leq C'\,\|u_{n,e}^l\|^2_{L^2(\mathbb{R}^2)}\int_1^\infty \frac{dt}{|t|^{q+1}}$, C' being a constant and the last integral being convergent since $q \geq 3$, resulting in the uniform boundedness of $\int_0^\infty \dfrac{E_n^l(t)}{|t|^{q+1}}\,dt$. Besides, $\int_{\mathbb{R}} \dfrac{E_n^l(t)}{|t|^{q+1}}\,dt = \int_{\mathbb{R}} \frac{1}{|h|^{q+1}}\int_{\mathbb{R}^2} |u_{n,e}^l(x+he_1) - 2u_{n,e}^l(x) + u_{n,e}^l(x-he_1)|^2\,dx\,dh = \int_{\mathbb{R}} \frac{1}{|h|^{q+1}}\|\tau_{he_1}u_{n,e}^l - 2u_{n,e}^l + \tau_{-he_1}u_{n,e}^l\|^2_{L^2(\mathbb{R}^2)}\,dh = \int_{\mathbb{R}} \frac{1}{|h|^{q+1}}\int_{\mathbb{R}^2} |e^{2i\pi h\xi_1} - 2 + e^{-2i\pi h\xi_1}|^2 |\mathcal{F}(u_{n,e}^l)(\xi)|^2\,d\xi\,dh$ by Plancherel theorem ($\tau_.$ denoting the usual translation operator). Then one can prove that $\int_{\mathbb{R}} \dfrac{E_n^l(t)}{|t|^{q+1}}\,dt = C''\int_{\mathbb{R}^2} |\mathcal{F}(u_{n,e}^l)(\xi)|^2|\xi_1|^q \int_{\mathbb{R}} \frac{\sin^4(u)}{|u|^{q+1}}\,du\,d\xi \leq C$, (the constant C may change line to line). The generalized integral in u converges if and only if $q \in [3,4[$. By using the same arguments in the other direction (e_2), we get that $|\xi|^{\frac{q}{2}}\mathcal{F}(u_{n,e}^l) \in L^2(\mathbb{R}^2)$ and so $u_{n,e}^l \in H^{\frac{q}{2}}(\mathbb{R}^2)$ (being a Hilbert space) and is uniformly bounded for the associated norm with $q \in [3,4[$. There exists a subsequence still denoted by $u_{n,e}^l$ weakly converging to $\tilde{u}_n$ in $H^s(\mathbb{R}^2)$ with $s = \frac{q}{2}$. Besides, we know that $u_{n,e}^l = u_n^l$ on Ω and $D^{(1,0)}u_{n,e}^l = (D^{(1,0)}u_n^l)_e = D^{(1,0)}u_n^l$ on Ω, and $D^{(0,1)}u_{n,e}^l = (D^{(0,1)}u_n^l)_e = D^{(0,1)}u_n^l$ on Ω. Thus,

$$\begin{aligned}\|u_n^l\|^2_{W^{s,2}(\Omega)} &= \|u_n^l\|^2_{W^{1,2}(\Omega)} + \int_\Omega\int_\Omega \frac{|\nabla u_n^l(x) - \nabla u_n^l(y)|^2}{|x-y|^{2s}}\,dx\,dy\\ &\leq C + \int_{\mathbb{R}^2}\int_{\mathbb{R}^2} \frac{|\nabla u_{n,e}^l(x) - \nabla u_{n,e}^l(y)|^2}{|x-y|^{2s}}\,dx\,dy,\end{aligned}$$

with C independant of l. From [28, Lemma 4.33, p. 200], we know that

$$\begin{aligned}
&\int_{\mathbb{R}^2}\int_{\mathbb{R}^2} \frac{|\nabla u_{n,e}^l(x) - \nabla u_{n,e}^l(y)|^2}{|x-y|^{2s}}\,dx\,dy < \infty \\
\Leftrightarrow &\int_{\mathbb{R}}\int_{\mathbb{R}^2} \frac{|\nabla u_{n,e}^l(x) - \nabla u_{n,e}^l(x+he_1)|^2}{|h|^{2s-1}}\,dx\,dh < \infty
\end{aligned}$$

and $\int_{\mathbb{R}}\int_{\mathbb{R}^2} \frac{|\nabla u_{n,e}^l(x) - \nabla u_{n,e}^l(x+he_2)|^2}{|h|^{2s-1}}\,dx\,dh < \infty$. Let us now prove that $\int_{\mathbb{R}}\int_{\mathbb{R}^2} \frac{|\nabla u_{n,e}^l(x) - \nabla u_{n,e}^l(x+he_1)|^2}{|h|^{2s-1}}\,dx\,dh < \infty$ and

$$\int_{\mathbb{R}}\int_{\mathbb{R}^2} \frac{|\nabla u_{n,e}^l(x) - \nabla u_{n,e}^l(x+he_2)|^2}{|h|^{2s-1}}\,dx\,dh < \infty$$

independently of l.
We have

$$\begin{aligned}
&\int_{\mathbb{R}} \frac{1}{|h|^{2s-1}} \|\tau_{he_1}\nabla u_{n,e}^l - \nabla u_{n,e}^l\|_{L^2(\mathbb{R}^2)}^2\,dh \\
&\quad = \bar{C}\int_{\mathbb{R}} \frac{\sin^2(u)}{|u|^{2s-1}} \int_{\mathbb{R}^2} |\xi_1|^{2s-2}\,(|\xi_1|^2 + |\xi_2|^2)|\mathcal{F}(u_{n,e}^l)(\xi)|^2\,d\xi\,du \\
&\quad \leq C\|u_{n,e}^l\|_{H^s(\mathbb{R}^2)}^2,
\end{aligned}$$

by using Plancherel theorem and with C independant of l. By doing the same computations in the other direction, we prove that $\|u_n^l\|_{W^{s,2}(\Omega)}$ is uniformly bounded and so up to a subsequence, $u_n^l \underset{l\to+\infty}{\rightharpoonup} \overline{u_n}$ in $W^{s,2}(\Omega) \subset W^{1,2}(\Omega)$. As $W^{s,2}(\Omega) \underset{c}{\circlearrowleft} \mathcal{C}_b^{0,\lambda}(\Omega)$ with $\lambda < s-1$, then u_n^l strongly converges to $\overline{u_n}$ in $\mathcal{C}_b^{0,\lambda}(\Omega)$ and so pointwise everywhere on Ω.
Then $\tilde{u}_n = \overline{u_n}$ on Ω and $\overline{u_n} = 0$ on $\partial\Omega$, by uniqueness of the weak limit.
Now, $H^s(\mathbb{R}^2) \circlearrowleft L^2(\mathbb{R}^2) \circlearrowleft \mathcal{S}'(\mathbb{R}^2) \circlearrowleft \mathcal{D}'(\mathbb{R}^2)$ with continuous imbeddings. $\forall \varphi \in \mathcal{D}(\mathbb{R}^2)$,

$$\underbrace{\int_{\mathbb{R}^2} (u_{n,e}^l - \tilde{u}_n)\,\varphi\,dx}_{\underset{l\to+\infty}{\longrightarrow}0} = \underbrace{\int_{\Omega} (u_n^l - \overline{u_n})\,\varphi\,dx}_{\underset{l\to+\infty}{\longrightarrow}0} + \int_{\mathbb{R}^2\setminus\Omega} (u_{n,e}^l - \tilde{u}_n)\,\varphi\,dx.$$

Consequently, $\forall \varphi \in \mathcal{D}(\mathbb{R}^2)$, $\int_{\mathbb{R}^2\setminus\Omega} \tilde{u}_n \, \varphi \, dx = \int_{\mathbb{R}^2\setminus\bar{\Omega}} \tilde{u}_n \, \varphi \, dx = 0$, since $\tilde{u}_n \in H^s(\mathbb{R}^2) \circlearrowleft \mathcal{C}^0(\mathbb{R}^2)$. In particular, $\forall \varphi \in \mathcal{D}(\mathbb{R}^2 \setminus \bar{\Omega})$, $\int_{\mathbb{R}^2\setminus\bar{\Omega}} \tilde{u}_n \, \varphi \, dx = 0$, meaning that $\tilde{u}_n = 0$ on $\mathbb{R}^2 \setminus \bar{\Omega}$ in the sense of distributions. Due to the continuity of $\tilde{u}_n$, we deduce that $\tilde{u}_n = 0$ everywhere on $\mathbb{R}^2 \setminus \Omega$ and so $\tilde{u}_n = (\overline{u_n})_e$. By combining the previous results, we can say that $u^l_{n,e}$ converges pointwise everywhere to $(\overline{u_n})_e$ on $\mathbb{R}^2$.

- Classical arguments enable us to conclude that there exists a subsequence still denoted by $\vec{g_n}^{\,l}$ weakly converging to $\overline{\vec{g_n}}$ in $H(div)$.

2. **Lower semi-continuity of the functional**:

- Since $\nabla Q^l_n \overset{*}{\rightharpoonup} \nabla \overline{Q}_n$ in $L^\infty(\Omega)$ then

$$\|\nabla \overline{Q}_n\|_{L^\infty(\Omega)} \leq \liminf_{l\to+\infty} \|\nabla Q^l_n\|_{L^\infty(\Omega)}.$$

- Weak-$*$ convergence in $L^\infty(\Omega)$ implying weak convergence in $L^2(\Omega)$, $\|\nabla\overline{Q_n} - \overline{\vec{g_n}}\|^2_{L^2(\Omega)} \leq \liminf_{l\to+\infty} \|\nabla Q^l_n - \vec{g_n}^{\,l}\|^2_{L^2(\Omega)}$.
- $\mathcal{G}_\varepsilon$ is convex and strongly lower semi-continuous in $H^1(\Omega)$ and so weakly lower semi-continuous in $H^1(\Omega)$.
- $\|f - \overline{u_n} - \operatorname{div} \overline{\vec{g_n}}\|^2_{L^2(\Omega)} \leq \liminf_{l\to+\infty} \|f - u^l_n - \operatorname{div}\vec{g_n}^{\,l}\|^2_{L^2(\Omega)}$.
- Let us consider $h : \Omega\times\mathbb{R}\times\mathbb{R}^2 \to \mathbb{R}$, $(x, v, w) \mapsto (v(x)^2+\lambda_\varepsilon)|w(x)|^2$. Since $v^l_{1,n} \underset{l\to+\infty}{\longrightarrow} \overline{v_{1,n}}$ in $L^2(\Omega)$, $\nabla u^l_n \underset{l\to+\infty}{\rightharpoonup} \nabla\overline{u_n}$ in $L^2(\Omega, \mathbb{R}^2)$, since h is continuous with respect to (v, w) and measurable on Ω for almost every $(v, w) \in \mathbb{R} \times \mathbb{R}^2$, for each (x, v), h is convex with respect to w, $\forall (v, w) \in \mathbb{R} \times \mathbb{R}^2$, $\forall x \in \Omega$ a.e., $h(x, v, w) \geq 0 \in L^1(\Omega)$ and $\liminf_{l\to+\infty} \int_\Omega ((v^l_{1,n}(x))^2 + \lambda_\varepsilon)|\nabla u^l_n|^2 \, dx < +\infty$, then $\int_\Omega (\overline{v_{1,n}}^2 + \lambda_\varepsilon)|\nabla\overline{u_n}|^2 \, dx \leq \liminf_{l\to+\infty} \int_\Omega ((v^l_{1,n})^2 + \lambda_\varepsilon)|\nabla u^l_n|^2 \, dx$ (see [13]).
- $v^l_{2,n} \underset{l\to+\infty}{\longrightarrow} \overline{v_{2,n}}$ in $L^2(\Omega)$, therefore $v^l_{2,n,e} \underset{l\to+\infty}{\longrightarrow} (\overline{v_{2,n}})_e$ in $L^2(\mathbb{R}^2)$ (since from [18, Theorem IX.7, (ii), p. 158], $\|v^l_{2,n,e} - (\overline{v_{2,n}})_e\|_{L^2(\mathbb{R}^2)} \leq \tilde{C}\, \|v^l_{2,n} - \overline{v_{2,n}}\|_{L^2(\Omega)}$, $\tilde{C}$ depending only on Ω) and so pointwise almost everywhere in $\mathbb{R}^2$ (up to a subsequence). We deduce that $((v^l_{2,n,e}(x))^2 + \kappa_\varepsilon)\frac{|u^l_{n,e}(x+he_i)-2u^l_{n,e}(x)+u^l_{n,e}(x-he_i)|^2}{|h|^4}\rho_n(h) \underset{l\to+\infty}{\longrightarrow} ((\overline{v_{2,n}})_e(x)^2 + \kappa_\varepsilon)\frac{|(\overline{u_n})_e(x+he_i)-2(\overline{u_n})_e(x)+(\overline{u_n})_e(x-he_i)|^2}{|h|^4}\rho_n(h)$, $i \in \{1, 2\}$, for all $h \in \mathbb{R}$ and almost all $x \in \mathbb{R}^2$.

Using Fatou's lemma twice, we deduce that $\int_{\mathbb{R}^2}\int_{\mathbb{R}}((\overline{v_{2,n}})_e(x)^2 + \kappa_\varepsilon)\frac{|(\overline{u_n})_e(x+he_i)-2(\overline{u_n})_e(x)+(\overline{u_n})_e(x-he_i)|^2}{|h|^4}\rho_n(h)\,dh\,dx \leq \liminf_{l\to+\infty}\int_{\mathbb{R}^2}\int_{\mathbb{R}} ((v_{2,n,e}^l(x))^2 + \kappa_\varepsilon)\frac{|u_{n,e}^l(x+he_1)-2u_{n,e}^l(x)+u_{n,e}^l(x-he_1)|^2}{|h|^4}\rho_n(h)\,dh\,dx$, $i \in \{1,2\}$.

This concludes the proof. □

We now turn to the part dedicated to numerical experiments related to the local problem. The numerical analysis of the algorithm related to the nonlocal model will be the core of a future paper.

4. Numerical experiments

4.1. Sketch of the algorithm

In this section, we briefly describe the main steps of our algorithm for the sake of reproducibility, and make qualitative comments. We recall that

$$\begin{cases} v_1 &= \dfrac{\frac{\alpha-\beta}{2\varepsilon} + 2(\alpha-\beta)\varepsilon\Delta v_1}{2\xi_\varepsilon|\nabla u|^2 + \frac{\alpha-\beta}{2\varepsilon}}, \quad v_2 = \dfrac{\frac{\beta}{2\varepsilon} + 2\beta\varepsilon\Delta v_2}{2\rho|\nabla^2 u|^2 + \frac{\beta}{2\varepsilon}}, \\ u &= (f - \operatorname{div}\vec{g}) - \rho\,\frac{\partial^2}{\partial x_1^2}\left(v_2^2\,\frac{\partial^2 u}{\partial x_1^2}\right) - \rho\,\frac{\partial^2}{\partial x_2^2}\left(v_2^2\,\frac{\partial^2 u}{\partial x_2^2}\right) \\ & \quad -2\rho\,\frac{\partial^2}{\partial x_1\partial x_2}\left(v_2^2\,\frac{\partial^2 u}{\partial x_1\partial x_2}\right) + \xi_\varepsilon\operatorname{div}(v_1^2\,\nabla u). \end{cases}$$

These equations can be interpreted as follows: when v_1 (respectively v_2) is close to 0 at some point, the role of the diffusion term $\operatorname{div}(v_1^2\,\nabla u)$ (resp. $\frac{\partial^2}{\partial x_i\partial x_j}\left(v_2^2\,\frac{\partial^2 u}{\partial x_i\partial x_j}\right)$, $i,j \in \{1,2\}$) is cut, yielding not oversmoothed regions along edges or fine structures. If on the contrary v_1 or v_2 is close to 1 at some point, there is diffusion in u at that point to obtain a smooth approximation. If $|\nabla u|$ is close to 0 at some point (resp. $|\nabla^2 u|^2$), then v_1 (resp. v_2) is close to 1, enhancing the regularization process. If on the contrary $|\nabla^2 u|$ is large, v_2 is close to 0 with a very small diffusion coefficient ($\simeq \frac{\beta\,\varepsilon}{\rho\,|\nabla^2 u|^2}$).

The algorithm consists in alternatively solving the Euler-Lagrange equations related to each unknown and presented in Section 2. We use a time-dependent scheme in $u = u(x_1,x_2,t)$ and $Q = Q(x_1,x_2,t)$ (nonlinear over-relaxation method, see [22, Section 4]), and a stationary semi-implicit fixed-point scheme in $v_1 = v_1(x_1,x_2)$, $v_2 = v_2(x_1,x_2)$ and $\vec{g} = \vec{g}(x_1,x_2)$. At the boundary, we extend u by reflection outside the domain, and a simple boundary condition for $\vec{g}$, $v_1 - 1$, and $v_2 - 1$ would be Dirichlet boundary conditions (and so Neumann boundary condition for Q), which appears to work well in practice.

Let $\Delta x_1 = \Delta x_2 = h = 1$ be the space step, let Δt be the time step, and let $f_{i,j}$, $u^n_{i,j}$, $Q^n_{i,j}$, $v^n_{1,i,j}$, $v^n_{2,i,j}$, $\vec{g}^n_{i,j} = (g^n_{1,i,j}, g^n_{2,i,j})^t$ be the discrete versions of f, u, Q, v_1, v_2 and $\vec{g}$ at iteration $n \geq 0$, for $1 \leq i \leq M$, $1 \leq j \leq N$.

Initialization: $u^0 = f$, $\vec{g}^0 = \vec{0}$, $Q^0 = 0$, $v^0_1 = 1$ and $v^0_2 = 1$.

Algorithm: For $n \geq 1$, compute and **repeat to steady state**:

$$|\nabla u^n|^2_{i,j} = (u^n_{i+1,j} - u^n_{i,j})^2 + (u^n_{i,j+1} - u^n_{i,j})^2,$$

$$v^{n+1}_{1,i,j} = \frac{\frac{(\alpha-\beta)}{2\varepsilon} + 2(\alpha-\beta)\varepsilon\,(v^n_{1,i+1,j} + v^n_{1,i-1,j} + v^n_{1,i,j+1} + v^n_{1,i,j-1} - 4v^{n+1}_{1,i,j})}{2\xi_\varepsilon\,|\nabla u^n|^2_{i,j} + \frac{(\alpha-\beta)}{2\varepsilon}},$$

$$|\nabla^2 u^n|^2_{i,j} = (u^n_{i+1,j} - 2u^n_{i,j} + u^n_{i-1,j})^2 + 2\,(u^n_{i+1,j+1} - u^n_{i+1,j} - u^n_{i,j+1} + u^n_{i,j})^2 + (u^n_{i,j+1} - 2u^n_{i,j} + u^n_{i,j-1})^2,$$

$$v^{n+1}_{2,i,j} = \frac{\frac{\beta}{2\varepsilon} + 2\beta\varepsilon\,(v^n_{2,i+1,j} + v^n_{2,i-1,j} + v^n_{2,i,j+1} + v^n_{2,i,j-1} - 4v^{n+1}_{2,i,j})}{2\rho\,|\nabla^2 u^n|^2_{i,j} + \frac{\beta}{2\varepsilon}},$$

$$\begin{aligned}
\frac{u^{n+1}_{i,j} - u^n_{i,j}}{\Delta t} &= (f_{i,j} - u^n_{i,j} - \frac{g^n_{1,i,j+1} - g^n_{1,i,j-1}}{2} - \frac{g^n_{2,i+1,j} - g^n_{2,i-1,j}}{2}) \\
&+ \xi_\varepsilon \left[(v^{n+1}_{1,i,j})^2\,(u^n_{i,j+1} - u^n_{i,j}) - (v^{n+1}_{1,i,j-1})^2\,(u^n_{i,j} - u^n_{i,j-1})\right] \\
&+ \xi_\varepsilon \left[(v^{n+1}_{1,i,j})^2\,(u^n_{i+1,j} - u^n_{i,j}) - (v^{n+1}_{1,i-1,j})^2\,(u^n_{i,j} - u^n_{i-1,j})\right] \\
&- \rho \left[(v^{n+1}_{2,i,j+1})^2\,(u^n_{i,j+2} - 2u^n_{i,j+1} + u^n_{i,j}) - 2\,(v^{n+1}_{2,i,j})^2\,(u^n_{i,j+1} - 2u^n_{i,j} + u^n_{i,j-1})\right. \\
&\left. + (v^{n+1}_{2,i,j-1})^2\,(u^n_{i,j} - 2u^n_{i,j-1} + u^n_{i,j-2})\right] - \rho \left[(v^{n+1}_{2,i+1,j})^2\,(u^n_{i+2,j} - 2u^n_{i+1,j} + u^n_{i,j})\right. \\
&\left. -2\,(v^{n+1}_{2,i,j})^2\,(u^n_{i+1,j} - 2u^n_{i,j} + u^n_{i-1,j}) + (v^{n+1}_{2,i-1,j})^2\,(u^n_{i,j} - 2u^n_{i-1,j} + u^n_{i-2,j})\right] \\
&- 2\,\rho \left[(v^{n+1}_{2,i+1,j+1})^2\,(u^n_{i+2,j+2} - u^n_{i+1,j+2} - u^n_{i+2,j+1} + u^n_{i+1,j+1})\right. \\
&- (v^{n+1}_{2,i,j+1})^2\,(u^n_{i+1,j+2} - u^n_{i,j+2} - u^n_{i+1,j+1} + u^n_{i,j+1}) \\
&- (v^{n+1}_{2,i+1,j})^2\,(u^n_{i+2,j+1} - u^n_{i+1,j+1} - u^n_{i+2,j} + u^n_{i+1,j}) \\
&\left. +(v^{n+1}_{2,i,j})^2\,(u^n_{i+1,j+1} - u^n_{i,j+1} - u^n_{i+1,j} + u^n_{i,j})\right],
\end{aligned}$$

and equations derived in the same way for g^n_1, g^n_2 and Q^n.

An alternating minimization procedure is thus performed (see [19]), yielding convergence properties. More precisely, starting with initial guess $v^0_1 \in S \subset \mathbb{R}^{M\times N}$, $v^0_2 \in S \subset \mathbb{R}^{M\times N}$, $u^0 \in X \subset \mathbb{R}^{M\times N}$, $\vec{g}^0 \in Z \subset (\mathbb{R}^{M\times N})^2$

and $Q^0 \in Y \subset \mathbb{R}^{M\times N}$, we successively obtain the sequence of conditional minimizers by solving

$$\begin{aligned}
v_1^{(k+1)} &\in \operatorname*{arg\,min}_{v_1\in S} \mathcal{F}_\varepsilon(u^{(k)}, \vec{g}^{(k)}, Q^{(k)}, v_1, v_2^{(k)}),\\
v_2^{(k+1)} &\in \operatorname*{arg\,min}_{v_2\in S} \mathcal{F}_\varepsilon(u^{(k)}, \vec{g}^{(k)}, Q^{(k)}, v_1^{(k+1)}, v_2),\\
u^{(k+1)} &\in \operatorname*{arg\,min}_{u\in X} \mathcal{F}_\varepsilon(u, \vec{g}^{(k)}, Q^{(k)}, v_1^{(k+1)}, v_2^{(k+1)}),\\
\vec{g}^{(k+1)} &\in \operatorname*{arg\,min}_{\vec{g}\in Z} \mathcal{F}_\varepsilon(u^{(k+1)}, \vec{g}, Q^{(k)}, v_1^{(k+1)}, v_2^{(k+1)}),\\
Q^{(k+1)} &\in \operatorname*{arg\,min}_{Q\in Y} \mathcal{F}_\varepsilon(u^{(k+1)}, \vec{g}^{(k+1)}, Q, v_1^{(k+1)}, v_2^{(k+1)}),
\end{aligned}$$

for $k \geq 0$. We consecutively prove:

(i) The monotonicity property

$$\mathcal{F}_\varepsilon(u^{(k+1)}, \vec{g}^{(k+1)}, Q^{(k+1)}, v_1^{(k+1)}, v_2^{(k+1)}) \leq \mathcal{F}_\varepsilon(u^{(k)}, \vec{g}^{(k)}, Q^{(k)}, v_1^{(k)}, v_2^{(k)}),$$

$\forall k \in \mathbb{N}$, ensuring that the sequence $\left\{\mathcal{F}_\varepsilon(u^{(k)}, \vec{g}^{(k)}, Q^{(k)}, v_1^{(k)}, v_2^{(k)})\right\}$ converges.

(ii) For any converging subsequence $(u^{(\Psi(k))}, \vec{g}^{(\Psi(k))}, Q^{(\Psi(k))}, v_1^{(\Psi(k))}, v_2^{(\Psi(k))})$ of $(u^{(k)}, \vec{g}^{(k)}, Q^{(k)}, v_1^{(k)}, v_2^{(k)})$ generated by the algorithm with

$$(u^{(\Psi(k))}, \vec{g}^{(\Psi(k))}, Q^{(\Psi(k))}, v_1^{(\Psi(k))}, v_2^{(\Psi(k))}) \underset{k\to+\infty}{\longrightarrow} (u^*, \vec{g}^*, Q^*, v_1^*, v_2^*),$$

the following holds:

$$\begin{aligned}
&\forall u \in X,\ \mathcal{F}_\varepsilon(u^*, \vec{g}^*, Q^*, v_1^*, v_2^*) \leq \mathcal{F}_\varepsilon(u, \vec{g}^*, Q^*, v_1^*, v_2^*),\\
&\forall Q \in Y,\ \mathcal{F}_\varepsilon(u^*, \vec{g}^*, Q^*, v_1^*, v_2^*) \leq \mathcal{F}_\varepsilon(u^*, \vec{g}^*, Q, v_1^*, v_2^*),\\
&\forall \vec{g} \in Z,\ \mathcal{F}_\varepsilon(u^*, \vec{g}^*, Q^*, v_1^*, v_2^*) \leq \mathcal{F}_\varepsilon(u^*, \vec{g}, Q^*, v_1^*, v_2^*),\\
&\forall v_1 \in S,\ \mathcal{F}_\varepsilon(u^*, \vec{g}^*, Q^*, v_1^*, v_2^*) \leq \mathcal{F}_\varepsilon(u^*, \vec{g}^*, Q^*, v_1, v_2^*),\\
&\forall v_2 \in S,\ \mathcal{F}_\varepsilon(u^*, \vec{g}^*, Q^*, v_1^*, v_2^*) \leq \mathcal{F}_\varepsilon(u^*, \vec{g}^*, Q^*, v_1^*, v_2),
\end{aligned}$$

making $(u^*, \vec{g}^*, Q^*, v_1^*, v_2^*)$ a partial minimizer.

(iii) If $(u^{(k)}, \vec{g}^{(k)}, Q^{(k)}, v_1^{(k)}, v_2^{k)}) \underset{k\to+\infty}{\longrightarrow} (u^*, \vec{g}^*, Q^*, v_1^*, v_2^*)$, then $(u^*, \vec{g}^*, Q^*, v_1^*, v_2^*)$ belongs to the set of all partial minimizers of the problem.
If $(u^{(k)}, \vec{g}^{(k)}, Q^{(k)}, v_1^{(k)}, v_2^{k)})$ does not converge, there exists a subsequence that converges to a partial minimizer of the problem.

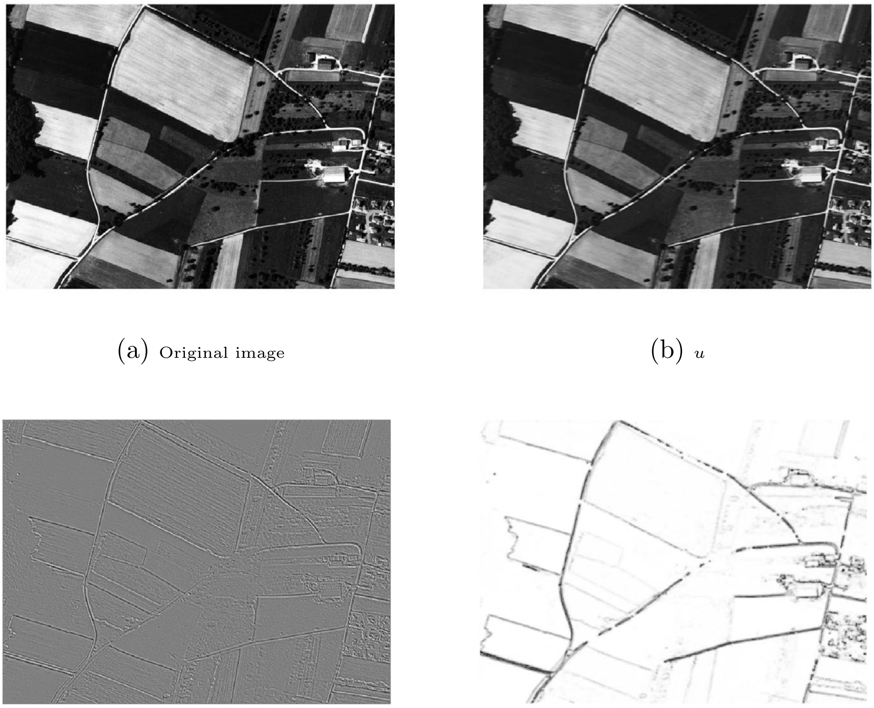

(a) Original image (b) u

(c) $v = \operatorname{div} \vec{g}$ (d) v_2

Figure 2: Road network extraction on an aerial scene: $\mu = 8$, $\xi_\varepsilon = 0$, $\alpha = \beta = 0.5$, $\rho = 5$, $\varepsilon = 0.5$, $\gamma = 0.5$, 10 iterations.

4.2. Numerical simulations

Experimental results on real datasets are now provided, resulting from the application of the above algorithm. The values of the parameters in the functional are chosen on the basis of the results of a number of experiments. We can nevertheless infer the behavior of some of them: less regularization (smaller α, β, ρ and ξ_ε) induces more edges/creases in v_1 and v_2 respectively. Also, a higher parameter μ balancing the L^∞-norm of $|\nabla Q|$ will lead to smaller scale features in the $v = \operatorname{div} \vec{g}$ component. The fine structures appear as contours along which the auxiliary variable v_2 is close to zero, while jumps appear as contours with larger thickness.

We start off with an application dedicated to road network detection on urban scenes. An aerial urban scene is depicted in Fig. 2 (A. Drogoul's courtesy, size of the image 652×892), together with its smooth approximation u

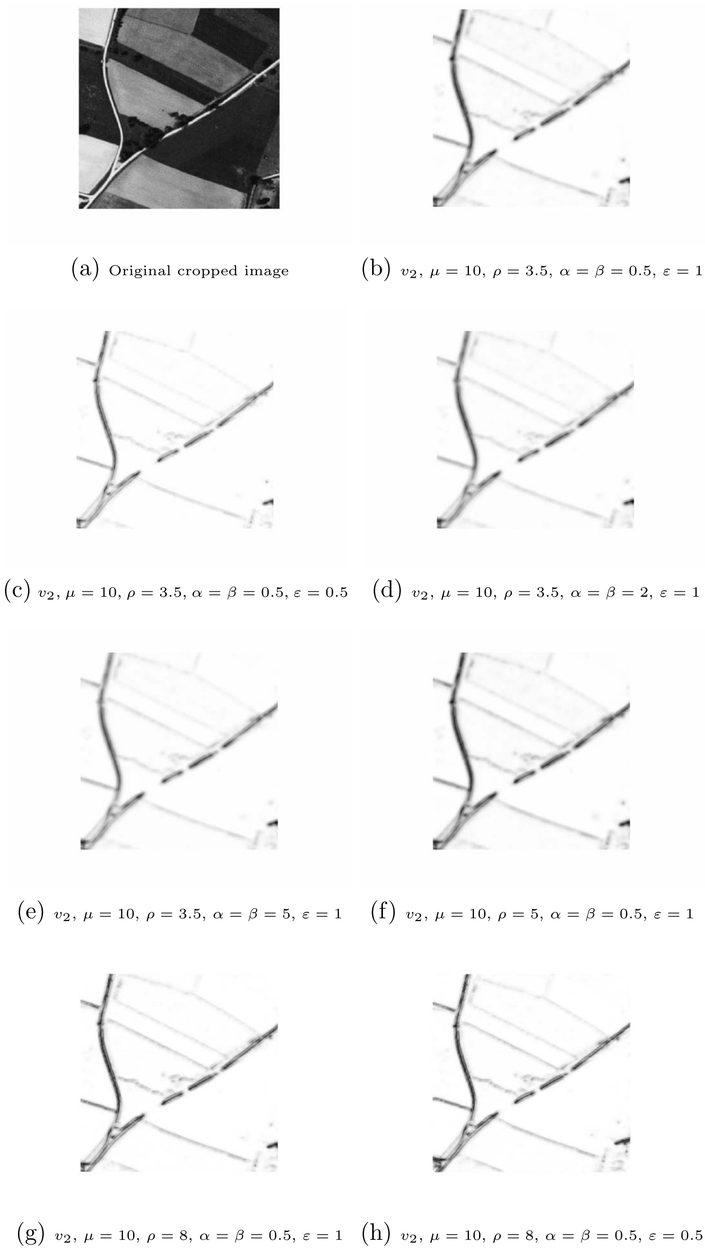

(a) Original cropped image
(b) v_2, $\mu = 10$, $\rho = 3.5$, $\alpha = \beta = 0.5$, $\varepsilon = 1$
(c) v_2, $\mu = 10$, $\rho = 3.5$, $\alpha = \beta = 0.5$, $\varepsilon = 0.5$
(d) v_2, $\mu = 10$, $\rho = 3.5$, $\alpha = \beta = 2$, $\varepsilon = 1$
(e) v_2, $\mu = 10$, $\rho = 3.5$, $\alpha = \beta = 5$, $\varepsilon = 1$
(f) v_2, $\mu = 10$, $\rho = 5$, $\alpha = \beta = 0.5$, $\varepsilon = 1$
(g) v_2, $\mu = 10$, $\rho = 8$, $\alpha = \beta = 0.5$, $\varepsilon = 1$
(h) v_2, $\mu = 10$, $\rho = 8$, $\alpha = \beta = 0.5$, $\varepsilon = 0.5$

Figure 3: Road network extraction on an aerial scene: effect of the parameters on the component v_2.

(a) Original image

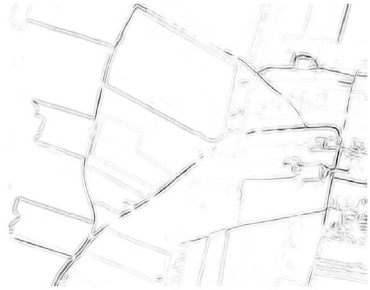

(b) Structures detected by the topological indicator

Figure 4: Road network extraction on an aerial scene with Aubert and Drogoul's topological gradient method.

in which small scale features have been removed (more precisely, u should be piecewise linear since the model involves second order penalization) and the auxiliary function v_2 that maps the fine structures of u. Function v_2 discriminates properly edges (i.e. discontinuities in the image function) that appear in light gray, from creases and filaments (i.e. road network here) that appear in dark gray. Small scale features are assimilated to oscillatory patterns having small G-norm and are thus well-captured in the $v = \operatorname{div} \vec{g}$ component (e.g., the rows in the fields are clearly extracted). The road network is clearly detected, while noise and texture are left in the $v = \operatorname{div} \vec{g}$ component. The most sensitive parameters are those related to regularization, namely ρ, α and β. The smaller parameters α and β are, the more edges/creases are present in the auxiliary function v_2. Parameter ρ acts on the thickness of the contours and on the range of function v_2: the higher ρ is, the closer to the value one contours representing fine structures are. Parameter ε also plays on the thickness and intensity of the contours, and is always set between 0.5 and 1. These elements are exemplified in Fig. 3 where various sets of parameters have been tested. We compare our results with those obtained by Aubert and Drogoul [9, 29] with the topological gradient (Fig. 4). We first observe that the topological gradient has the tendency to oversmooth the contours. Second, it does not properly discriminate the edges from the filaments and creases in terms of intensity for instance. At last, even if we tuned the algorithm adequately (in particular, a weighting parameter in their model influences the size of the detected structures), our algorithm detects more accurately the center of the road network. Another illustration devoted to filament/vessel-like structure detection is provided on Fig. 5 (size 338 $\times$

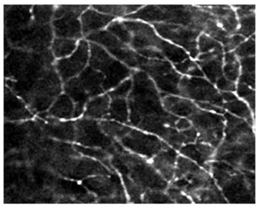

(a) Original image

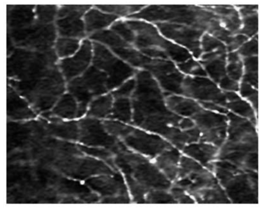

(b) u

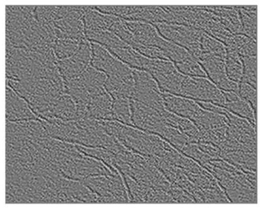

(c) $v = \operatorname{div} \vec{g}$

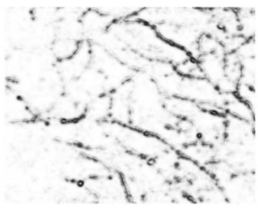

(d) v_2

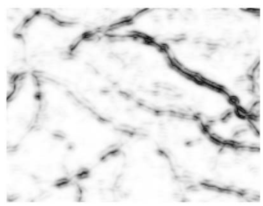

(e) v_2, zoom on a region of the image

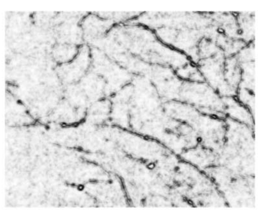

(f) v_2, when no decomposition is applied

Figure 5: Dendrite and axon extraction: $\mu = 1$, $\xi_\varepsilon = 0$, $\alpha = \beta = 0.1$, $\rho = 3.5$, $\varepsilon = 0.5$, $\gamma = 5$, 20 iterations.

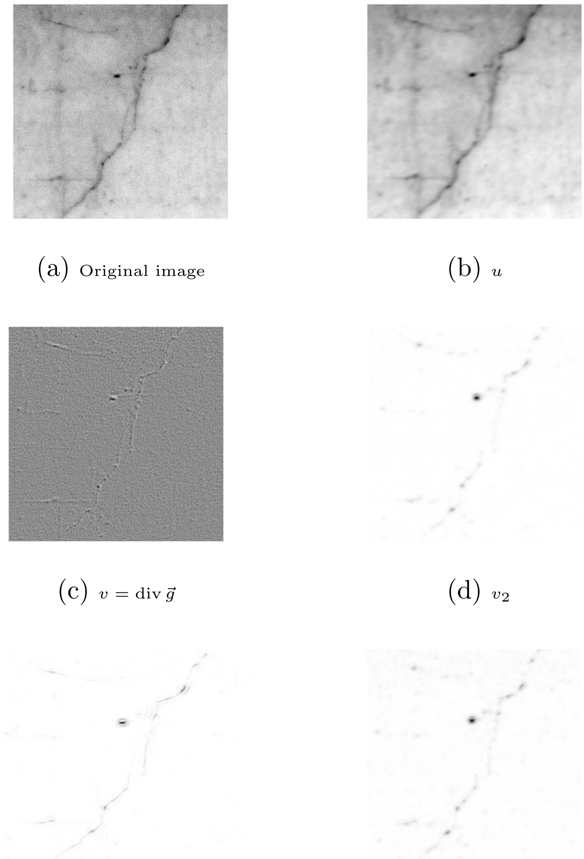

(a) Original image (b) u

(c) $v = \operatorname{div} \vec{g}$ (d) v_2

(e) Structures detected by the topological indicator (f) v_2, when no decomposition is applied

Figure 6: Crack detection: $\mu = 0.001$, $\xi_\varepsilon = 3.5$, $\alpha = 0.14$, $\beta = 0.07$, $\rho = 3.5$, $\varepsilon = 1$, $\gamma = 0.5$, 50 iterations.

436) and focuses on dendrite and axon detection (courtesy of A. Draugoul, https://sites.google.com/site/drogoulaudric/recherche). The skeleton of the dendrite network is well recovered, with in particular strong intensity in the middle of the dendrites. Also, to emphasize the role of the decomposition, we display the v_2 component when $\vec{g}$ and Q are removed from the model: we observe that spurious details (not related to filament structures) spoil this constituent. We now apply the proposed algorithm to crack detection, both on Fig. 6 (size 501 $\times$ 501) and 7 (size 285 $\times$ 429), courtesy of A. Drogoul. We depict the three main components of the decomposition/segmentation,

(a) Original image

(b) u

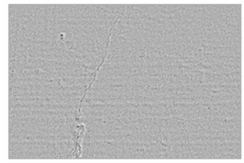

(c) $v = \operatorname{div} \vec{g}$

(d) v_2

(e) Structures detected by the topological indicator

Figure 7: Crack detection: $\mu = 0.001$, $\xi_\varepsilon = 3.5$, $\alpha = 0.14$, $\beta = 0.07$, $\rho = 3.5$, $\varepsilon = 1$, $\gamma = 0.5$, 50 iterations.

i.e., u, $v = \operatorname{div} \vec{g}$, v_2, as well as the results obtained with Aubert and Drogoul's topological gradient method. The cracks are correctly enhanced, the oscillatory patterns are well captured by the $v = \operatorname{div} \vec{g}$ component. Again, the role of the decomposition part of the algorithm is highlighted (Fig. 6) by depicting the obtained v_2 component when decomposition is turned off (spurious details are visible on the top of the image). Also, the linear piecewise nature of the component u in Fig. 7 is properly returned.

We conclude the paper with two applications dedicated to crack detection on bituminous surfacing Fig. 8 (size 231×650) and 9 (size 201×640), courtesy of CEREMA, France. The two considered slices of bitumen, in addition to long and thin cracks, exhibit high oscillatory patterns and white spots of varying sizes, which makes the straight application of our algorithm difficult. Indeed, in terms of scale, the crack and some of these spots could be comparable and could not be properly discriminated, resulting in superfluous information in the v_2 component. Think for instance of a white spot assimilated to a ball of radius 2 pixels (—if the image domain is the $n \times n$ discretized unit square, then the scale behaves like $\frac{1}{n}$—), and of a long thin crack of width 2 pixels and length k pixels ($k \gg 1$) leading to a similar scale.

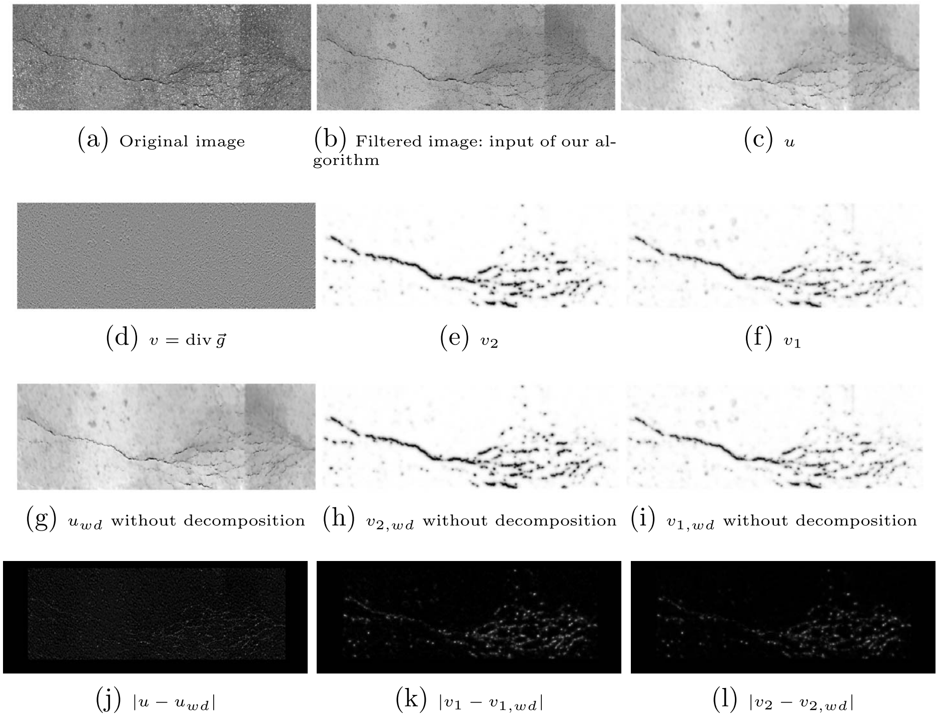

Figure 8: Crack detection: $\mu = 0.0001$, $\xi_\varepsilon = 3.5$, $\alpha = 0.14$, $\beta = 0.07$, $\rho = 3.5$, $\varepsilon = 1$, $\gamma = 0.9$, 270 iterations.

To circumvent this issue, a pre-processing step is applied. It consists in apprehending the problem first as an inpainting one ([1]), and by considering these white spots as missing parts of the image that need to be filled. This is achieved with the MATLAB® function **imfill** (https://fr.mathworks.com/help/images/ref/imfill.html —to fill holes in a grayscale image) applied to the inverse image, yielding an image that serves as input of our algorithm. In both cases, the cracks are well recovered in the v_2 component which does not include superfluous information. The edge detector v_1 also recovers parts of the crack but contains spurious information regarding the problem we address, such as asphalt defect boundaries. It thus justifies the use of a second order method.

Besides, Fig. 8-(g)-(h)-(i) and 9-(g)-(h)-(i) are the results obtained by minimizing the elliptic approximation of the Blake-Zisserman functional that is to say without considering the decomposition part. Thanks to Fig. 8-(j)-(k)-(l) and 9-(j)-(k)-(l) showing the absolute difference between both results,

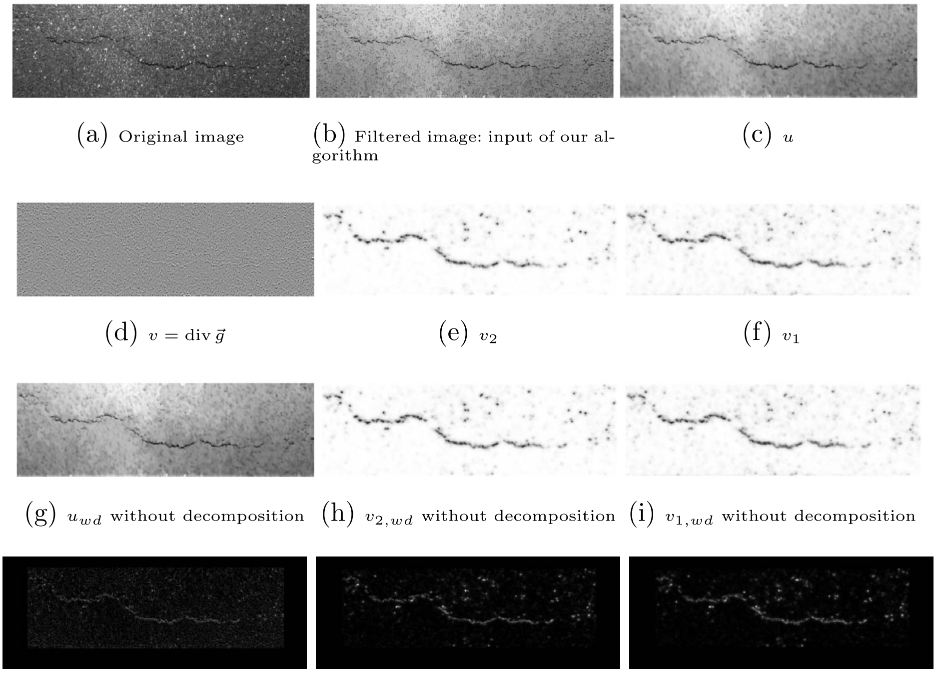

(a) Original image (b) Filtered image: input of our algorithm (c) u

(d) $v = \operatorname{div} \vec{g}$ (e) v_2 (f) v_1

(g) u_{wd} without decomposition (h) $v_{2,wd}$ without decomposition (i) $v_{1,wd}$ without decomposition

(j) $|u - u_{wd}|$ (k) $|v_1 - v_{1,wd}|$ (l) $|v_2 - v_{2,wd}|$

Figure 9: Crack detection: $\mu = 0.001$, $\xi_\varepsilon = 2.5$, $\alpha = 0.1$, $\beta = 0.05$, $\rho = 2.5$, $\varepsilon = 1$, $\gamma = 0.9$, 270 iterations.

we observe that u is less noisy with our method, v_1 and v_2 also exhibit better constrast with less superfluous information.

References

[1] Adam, R. D., Peter, P., Weickert, J., *Denoising by inpainting.* In Lauze, F., Dong, Y., Dahl, A. B. (eds) Scale Space and Variational Methods in Computer Vision: 6th International Conference, SSVM 2017, Kolding, Denmark, June 4–8, 2017, Proceedings, pp. 121–132. Springer International Publishing (2017).

[2] Ambrosio, L., Tortorelli, V. M., Approximation of Functionals Depending on Jumps by Elliptic Functionals via Γ-convergence. *Commun. Pur. Appl. Math.* **43** (1990), 999–1036. MR1075076

[3] Ambrosio, L., Tortorelli, V. M., On the Approximation of Free Discontinuity Problems. *B. Unione Mat. Ital.* (1992), 105–123. MR1164940

[4] Ambrosio, L., Faina, L., March, R., Variational Approximation of a Second Order Free Discontinuity Problem in Computer Vision. *SIAM J. Math. Anal.* **32(6)** (2001), 1171–1197. MR1856244

[5] Aronsson, G., Crandall, M., Juutinen, P., A Tour of the Theory of Absolutely Minimizing Functions. *B. Am. Math. Soc.* **41** (2004), 439–505. MR2083637

[6] Aubert, G., Aujol, J.-F., Blanc-Féraud, L., Detecting Codimension–Two Objects in an Image with Ginzburg-Landau Models. *Int. J. Comput. Vision* **65(1)** (2005), 29–42.

[7] Aubert, G., Aujol, J.-F., Modeling Very Oscillating Signals. Applications to Image Processing. *Appl. Math. Opt.* **51(2)** (2005), 163–182. MR2117231

[8] Aubert, G., Kornprobst, P., Can the nonlocal characterization of Sobolev spaces by Bourgain et al. be useful for solving variational problems? *SIAM J. Numer. Anal.* **47(2)** (2009), 844–860. MR2485435

[9] Aubert, G., Drogoul, A., Topological Gradient for a Fourth Order Operator Used in Image Analysis. *ESAIM: COCV* **21(4)** (2015), 1120–1149. MR3395758

[10] Baudour, A., Aubert, G., Blanc-Féraud, L., *Detection and Completion of Filaments: A Vector Field and PDE Approach.* In: Sgallari, F., Murli, A., Paragios, N. (eds.) SSVM 2007. LNCS, vol. 4485, pp. 451–460. Springer, Heidelberg (2007).

[11] Bergounioux, M., Piffet, L., A second-order model for image denoising. *Set-Valued Var. Anal.* **18(3–4)** (2010), 277–306. MR2739580

[12] Bergounioux, M., Vicente, D., Parameter Selection in a Mumford-Shah Geometrical Model for the Detection of Thin Structures. *Acta Appl. Math.* **141(1)** (2016), 17–48. MR3447161

[13] Berkovitz, L., D., Lower Semicontinuity of Integral Functionals. *Trans. AMS* **192** (1974), 51–57. MR0348582

[14] Blake, A., Zisserman, A., *Visual Reconstruction.* MIT Press, Cambridge. (1989). MR0919733

[15] Boulanger, J., Elbau, P., Pontow, C., Scherzer, O., *Non-Local Functionals for Imaging.* In Bauschke, H. H., Burachik, R. S., Combettes, P. L., Elser, V., Luke, D. R., Wolkowicz, H. (eds) Fixed-Point Algorithms for Inverse Problems in Science and Engineering, pp. 131–154. Springer New York (2011). MR2858836

[16] Bourgain, J., Brezis, H., Mironescu, P., *Another look at Sobolev spaces.* In: Menaldi, J. L., Rofman, E., Sulem, A. (eds) Optimal Control and Partial Differential Equations, in honour of Professor Alain Bensoussan's 60^{th} Birthday, pp. 439–455 (2001). MR3586796

[17] Bredies, K., Kunisch, K., Pock, T., Total generalized variation. *SIAM J. Imaging Sci.* **3(3)** (2010), 492–526. MR2736018

[18] Brezis, H., *Analyse fonctionnelle.* Dunod Paris (2005). MR0697382

[19] Cai, X., Variational image segmentation model coupled with image restoration achievements. *Pattern Recognit.* **48(6)** (2015), 2029–2042.

[20] Carriero, M., Leaci, A., Tomarelli, F., *A Second Order Model In Image Segmentation: Blake & Zisserman Functional.* In: Variational Methods for Discontinuous Structures: Applications to image segmentation, continuum mechanics, homogenization, Birkhäuser Basel (1996), 57–72. MR1414488

[21] Carriero, M., Leaci, A., Tomarelli, F., Free Gradient Discontinuity and Image Inpainting. *J. Math. Sci.* **181(6)** (2012), 805–819. MR2870231

[22] Caselles, V., Morel, J.-M., Sbert, C., An Axiomatic Approach to Image interpolation. *IEEE T. Image Process.* **7(3)** (1998), 376–386. MR1669524

[23] Chambolle, A., Lions, P. L., Image recovery via total variation minimization and related problems. *Numer. Math.* **76** (1997), 167–188. MR1440119

[24] Chan, T., Marquina, A., Mulet, P., High-order total variation-based image restoration. *SIAM J. Sci. Comput.* **22(2)** (2001), 503–516. MR1780611

[25] Chan, T., Kang, S. H., Shen, J., Euler's elastica and curvature-based inpainting. *SIAM J. Appl. Math.* **63(2)** (2002), 564–592. MR1951951

[26] Dal Maso, G., *An Introduction to* Γ*-convergence.* Birkhäuser, Boston (1993). MR1201152

[27] Dávila, J., On an open question about functions of bounded variation. *Calc. Var. Partial Differential Equations* **15(4)** (2002), 519–527. MR1942130

[28] Demengel, F., Demengel, G., *Functional Spaces for the Theory of Elliptic Partial Differential Equations.* Springer London (2012). MR2895178

[29] Drogoul, A., Numerical Analysis of the Topological Gradient Method for Fourth Order Models and Applications to the Detection of Fine Structures in Imaging. *SIAM J. Imaging Sci.* **7(4)** (2014), 2700–2731. MR3291535

[30] Forcadel, N., Dislocation Dynamics with a Mean Curvature Term: Short Time Existence and Uniqueness. *Differ. Integral Equ.* **21(3–4)** (2008), 285–304. MR2484010

[31] Gilboa, G., Osher, S., Nonlocal operators with applications to image processing. *Multiscale Model. Simul.* **7(3)** (2008), 1005–1028. MR2480109

[32] Lellman, J., Papafitsoros, K., Schönlieb, C., Spector, D., Analysis and application of a non-local Hessian. *SIAM J. Imaging Sci.* **8(4)** (2015), 2161–2202. MR3404680

[33] Meyer, Y., Oscillating Patterns in Image Processing and Nonlinear Evolution Equations. *Amer. Math. Soc.* **22** (2002). MR1852741

[34] Mumford, D., Shah, J., Optimal Approximations by Piecewise Smooth Functions and Associated Variational Problems. *Commun. Pur. Appl. Math.* **42** (1989), 577–685. MR0997568

[35] Nemitz, O., Rumpf, M., Tasdizen, T., Whitaker, R., Anisotropic Curvature Motion for Structure Enhancing Smoothing of 3D MR Angiography Data. *J. Math. Imaging Vis.* **27(3)** (2007), 217–229. MR2325849

[36] Ponce, A. C., A new approach to Sobolev spaces and connections to Γ-convergence. *Calc. Var. Partial Differential Equations* **19(3)** (2004), 229–255. MR2033060

[37] Rochery, M., Jermyn, I. H., Zerubia, J., Higher Order Active Contours. *Int. J. Comput. Vision* **69(1)** (2006), 27–42.

[38] Spector, D., *Characterization of Sobolev and BV Spaces*. PhD thesis, Carnegie Mellon University (2011). MR2890078

[39] Stoica, R., Descombes, X., Zerubia, J., A Gibbs Point Process for Road Extraction from Remotely Sensed Images. *Int. J. Comput. Vision* **57(2)** (2004), 121–136.

[40] Strang, G., *L^1 and L^∞ Approximation of Vector Fields in the Plane.* In: Nonlinear Partial Differential Equations in Applied Science; Proceedings of The U.S.-Japan Seminar, 273–288. North-Holland (1982). MR0730248

[41] Zana, F., Klein, J.-C., Segmentation of Vesell-Like Patterns Using Mathematical Morphology and Curvature Evaluation. *IEEE T. Image Process.* **10(7)** (2001), 1010–1019.

[42] Zanetti, M., Vitti, A., *The Blake-Zisserman Model For Digital Surface Models Segmentation.* In: ISPRS Workshop Laser Scanning 2013, 355–360. ISPRS Annals of the Photogrammetry, Remote Sensing and Spatial Information Sciences (2013).

Noémie Debroux
Laboratoire de Mathématiques
Normandie Université
INSA de Rouen
685 avenue de l'Université
76801 Saint-Etienne-du-Rouvray Cedex
France
E-mail address: noemie.debroux@insa-rouen.fr

Carole Le Guyader
Laboratoire de Mathématiques
Normandie Université
INSA de Rouen
685 avenue de l'Université
76801 Saint-Etienne-du-Rouvray Cedex
France
E-mail address: carole.le-guyader@insa-rouen.fr

Luminita Vese
University of California, Los Angeles
Department of Mathematics
405 Hilgard Avenue
Los Angeles
CA 90095-1555
USA
E-mail address: lvese@math.ucla.edu

Received July 5, 2017